RSC Advances

A polynuclear hetero atom containing molecular organic scaffold to detect Al3+ ion through fluorescence Turn-On response

Journal:	*RSC Advances*
Manuscript ID:	RA-COM-05-2015-009693.R1
Article Type:	Communication
Date Submitted by the Author:	03-Jul-2015
Complete List of Authors:	Misra, Arvind; Banaras Hindu University, Chemistry; Banaras Hindu University, Chemistry Ali, Rashid; Banaras Hindu University,, Chemistry Razi, Syed; Banaras Hindu University,, Chemistry Srivastava, Priyanka; Banaras Hindu University,, Chemistry Shahid, Mohammad; Banaras Hindu University,, Chemistry

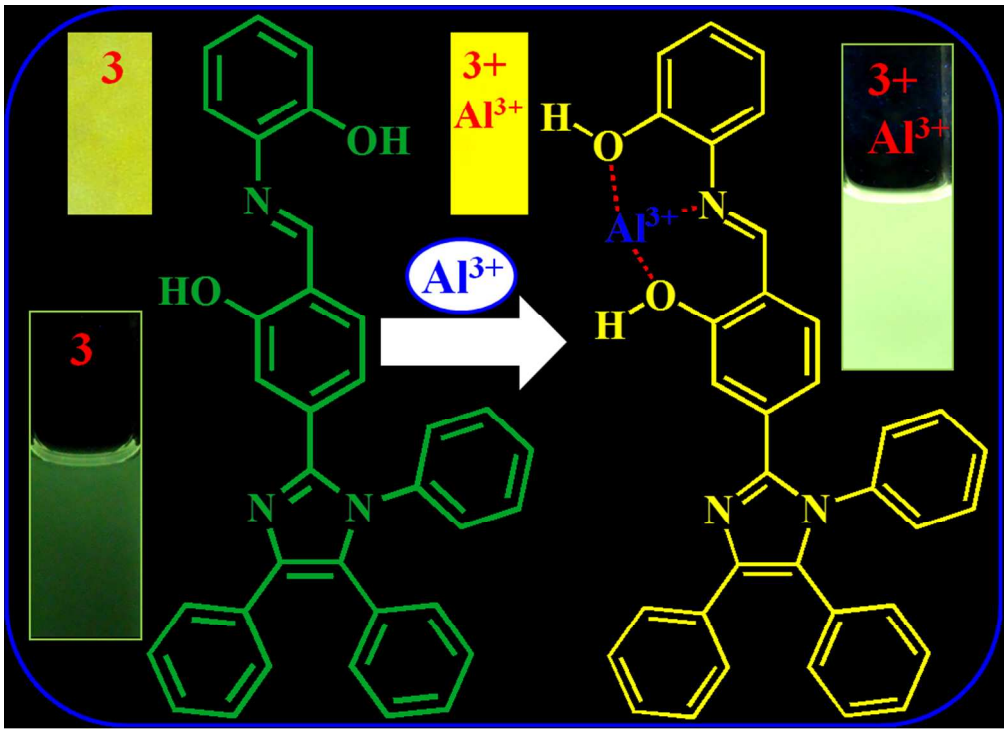

174x125mm (150 x 150 DPI)

Only for TOC

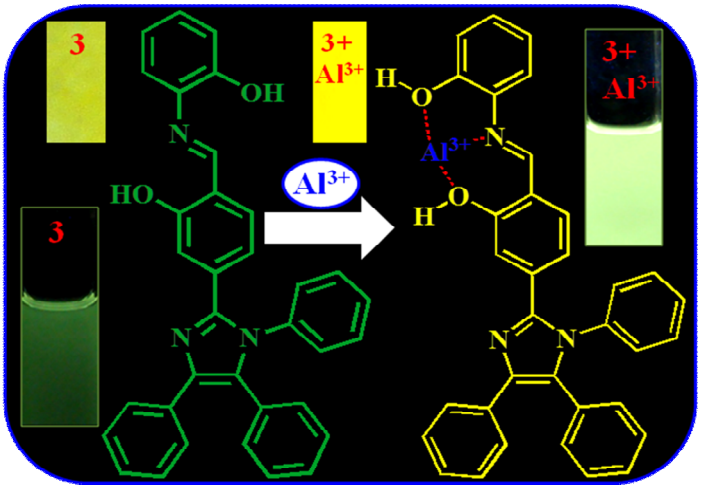

A polynuclear hetero atom containing molecular organic scaffold to detect Al^{3+} ion through fluorescence Turn-On response

Rashid Ali, Syed S. Razi, Priyanka Srivastava, Mohammad Shahid, and Arvind Misra*

Department of Chemistry, Faculty of Science, Banaras Hindu University, Varanasi – 221 005 UP INDIA

Corresponding author e-mail: arvindmisra2003@yahoo.com; amisra@bhu.ac.in

Abstract

A simple polynuclear hetero atom (*N* and *O*) containing molecular organic scaffold/probe, **3** has been designed and synthesized and explored as a potential chemosensor to detect Al^{3+} (22 nM; ~0.6 ppb) ion in HEPES buffer. Upon interaction with different metal ions and anions the weak emission intensity (switched –*Off*) of **3** (at 528 nm; λ_{ex}= 376 nm) enhanced significantly (switched–*On*; ~6.0 fold; Φ_{3+Al3+} = 0.07) only in the presence of Al^{3+} wherein, the color of solution changed from a naked-eye sensitive fluorescent dark green to bright yellow-green. The observed chelation enhanced fluorescence (CHEF) is attributable to restricted ESIPT and C=N isomerization processes due to complexation between the potential coordination sites (*N* and *O* atoms; Hard Base) of **3** and Al^{3+} (Hard Acid) in a 1:1 stoichiometry, consequently. The mechanism of interaction has been confirmed by the change in optical behaviors, $^{1}H/^{13}C$ NMR, FTIR, and ESI-MS spectroscopy data analysis. Moreover, chemosensor **3** has also been utilized to detect Al^{3+} in real water sample and on test paper strips.

Key Words: *Chemosensor, Al^{3+}, CHEF, ESIPT*

Introduction

The design and synthesis of new molecular scaffolds for the recognition and sensing of biologically and environmentally important species are always essential for practical research in various fields of science.[1] Among the available detection methods, chemosensors displaying ion induced fluorescence change are predominantly attractive in terms of sensitivity, selectivity, response time, simplicity, high degree of specificity and low detection limit.[2] The development of fluorescence turn-on chemosensors still remains a challenging task due to the fluorescence quenching effect of biologically important metal ions.[1-3] Thus, seeing the advantage of relatively higher detection sensitivity fluorescence turn-on probes, in comparison to turn-off probes, are in great demand in the recognition event of important metal ions, anions and biomolecules.[1-4]

Aluminium (Al^{3+}) is the third most prevalent (8.3% by weight) metallic element in the earth's crust and has wide application in our day-to-day life. Despite being a non-essential element in living organism people are widely exposed to aluminum by the frequent use of aluminium containing compounds in the form of food additives, paper and packing materials, water treatment, colors and pharmaceutical drugs.[5-6] The optimum concentration of Al^{3+} is crucial for human health, animals, aquatic biota and agricultural soil.[6,7] The unregulated concentration of aluminium in human body is believed to affect central nervous system, and cause diseases like Parkinson, Alzheimer, dementia, cancers and dialysis encephalopathy.[8] World Health Organization (WHO) considered aluminium as a food pollution source and limited Al^{3+} concentration to 200 $\mu g\ L^{-1}$ (7.41 mM) in drinking water, [3–10 mg daily intake of Al^{3+} ions] for a healthy human body.[9]

Further, the detection of Al^{3+} is challenging due to the some inherent associated properties such as, lack of specific spectroscopic characteristics, fluorescence quenching behavior, poor coordination and strong hydration abilities.[4a,10] Recently, some fluorescent chemosensors based on different photophysical mechanisms have been reported for Al^{3+} ion.[11,12] However, most of the chemosensors reported so far have faced limitation in the sense of aqueous medium compatibility of the probes, good photophysical behavior and most importantly interference of metal ions (like Cu^{2+}, Zn^{2+}, Fe^{3+}) and/or anions (like F^-, CH_3COO^-).[13] Therefore, it is highly desirable to develop some small synthetic molecular scaffolds/ fluorescent probes which can detect Al^{3+} selectively and sensitivity through a fluorescence turn-on response in the environment of competitive metal ions in a suitable complete or partial aqueous medium.

The structural motif for an efficient fluorescence signaling system involves three-components; a fluorophore, spacer and fluoroionophore/receptor, that are architected in a such fashion that the electronic communication between the fluorophore and receptor initially leads to low fluorescence (switched–*Off*) state, while upon interaction with a specific guest the communication between the two moieties break down to exhibit bright fluorescence (switched–*On*) in the medium.[14] Based on this unique design, we recently developed some sensitive molecular scaffolds to detect metal ions and anions in different medium.[15] Additionally, the structural motifs involving C=N isomerization and intramolecular proton transfer (ESIPT) exhibit weak emission in the ground state, and upon interaction with guest species are expected to display high-intensity, "turn-on" emission. Therefore, the signal transduction occurrence via chelation enhanced fluorescence and hindered ESIPT

processes are good strategy to detect metal ions. Based on this concept, in the present communication we wish to report design and synthesis of a new polynuclear hetero atom containing fluorescent chemosensor **3** to detect Al^{3+}ion. The chemosensor **3** has hard base type potential coordination sites in the form of *N* and *O* heteroatoms and is expected to tether the complementary hard acid species like, Al^{3+} ion. Moreover, to accomplish the objective of –C=*N*, isomerization and ESIPT process we designed probe **3** keeping aldimine and phenolic –OH function in a close proximity. Notably, upon interaction with different metal ions and anions **3** displayed naked-eye sensitive chelation enhanced fluorescence (CHEF) to detect Al^{3+} selectively in HEPES buffer, in which the emission intensity of chemosensor enhanced significantly, "turn-on response" due to restricted ESIPT and C=N isomerization processes.

2. RESULTS AND DISCUSSION

2.1. Synthesis, metal ion selectivity and fluorogenic response of probe 3

The multi-component reactions (MCRs) involving three or four different substrates has emerged as a powerful one-pot transformation strategy for the synthesis of chemically and biologically important diverse organic frameworks.[16] Therefore, we adopted MCR method to synthesis probe **3** as shown in Scheme 1. First compound **1** has been synthesized by reacting *m*-hydroxybenzaldehyde, benzil, aniline and ammonium acetate in acetic acid.[17a] Compound **1** was treated[17b] with $CHCl_3$ in KOH to get formyl derivative **2**, which was subsequently refluxed in ethanol with *o*-aminophenol using catalytic amount of iodine to obtain probe **3** as a red color solid in 80% yield. The products were characterized by ^{1}HNMR, ^{13}CNMR, FTIR and MS spectroscopy data (Figure S7-S11, Supporting Information).

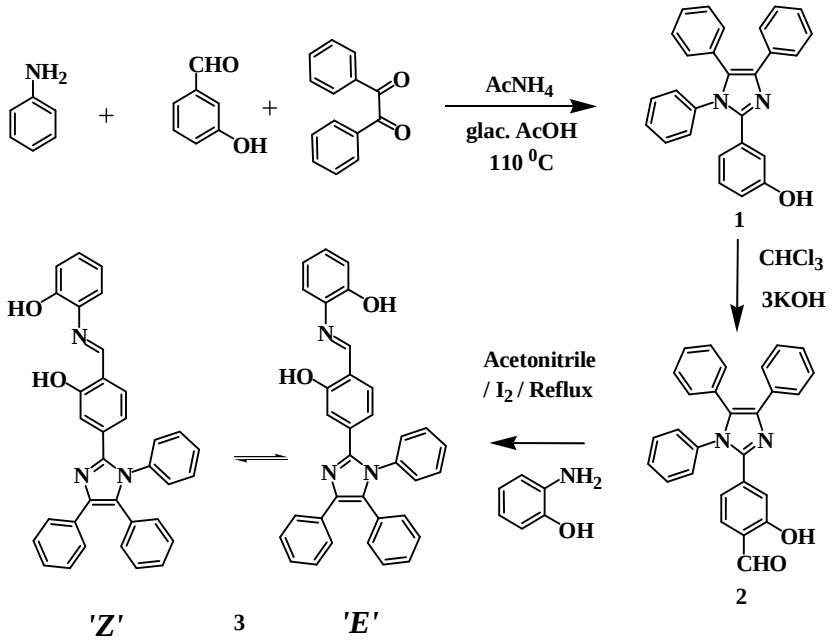

Scheme 1. Synthesis of probe **3**

The photophysical behavior of **3** and a complex, **3+Al^{3+}** have been studied in different solvents and water gradient systems (Table S1). The photophysical behavior displayed by probe **3** was found to be relatively good in ethanol and ethanol-water gradient systems hoever, overall analysis seems to be good in HEPES buffer. Therefore, the photophysical behavior of **3** in the absence and presence of different metal ions has been examined in HEPES buffer (10 mM, 50% THF/H_2O v/v, pH 7.04) through the absorption and emission spectroscopy. The electronic transition spectrum of **3** (10 μM) displayed (Figure 1) a low energy absorption band at 376 nm (ε = 1.41 x 10^4 $M^{-1}cm^{-1}$) and upon excitation at 376 nm displayed a weak emission band at 528 nm (Φ_3 = 0.006; Stokes shift 7656 cm^{-1}) due to the excited state intramolecular proton transfer (ESIPT) process. Upon addition of Al^{3+} (2.0 equiv) to a solution of **3**, the absorption band centered at 376 nm disappeared and two new bands appeared at 347 nm (ε = 1.31 x 10^4 $M^{-1}cm^{-1}$) and at 441 nm (ε = 4.58 x 10^3 $M^{-1}cm^{-1}$). Similarly, upon interaction with Al^{3+} (2.0 equiv) the weak emission intensity of **3** (at 528 nm; λ_{ex}= 376 nm) exhibited enhanced "turn-on" emission (~6.0 fold) in which quantum yield was increased (Φ_{3+Al3+} = 0.07) and the visual naked eye sensitive color of solution changed from a fluorescent dark green to a bright yellow-green color (Figure 1a, images). Additionally, upon interaction with other metal ions such as Na^+,

K^+, Ca^{2+}, Mg^{2+}, Co^{2+}, Ni^{2+}, Zn^{2+}, Fe^{2+}, Cr^{3+}, Pb^{2+}, Ag^+, Cd^{2+}, and Hg^{2+} (as their nitrate salts) the electronic transition spectrum of **3** remained almost consistent except with Hg^{2+}, Fe^{n+} and Cu^{2+} ions. The absorption spectrum of **3** upon interaction with Cu^{2+} showed new broad red shift band at 440 nm (ε = 9.33 x 10^3 $M^{-1}cm^{-1}$) with a shoulder at 339 nm (ε = 8.38 x 10^3 $M^{-1}cm^{-1}$) (Figure 1a). Similarly, **3** upon interaction with tested metal ions illustrated high selectivity for Al^{3+} but relatively weak emission intensity at 488 nm and 494 nm has been also observed with Hg^{2+} and Fe^{3+} ions, respectively and the color of the probe solution varied, accordingly. However, in comparison to a probable complex, **3**+Al^{3+} the other tested metal ions revealed almost negligible or weak fluorescence response (Figure 1b and 2, bar diagram).

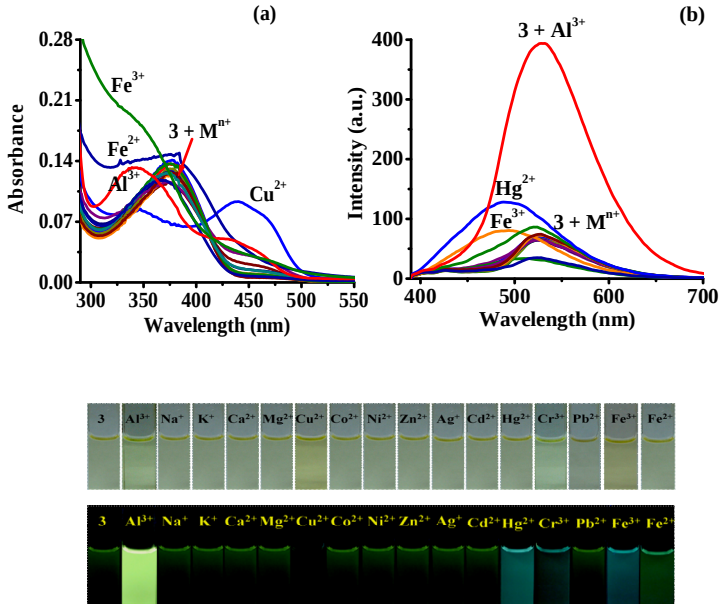

Figure 1: (a) Absorption and (b) emission spectra of **3** (10 μM) upon interaction with different metal ions (2.0 equiv) in HEPES buffer (50% H_2O/THF v/v, pH 7.04). **Images**: Chromogenic and fluorogenic (under UV light at 365 nm) response of **3** (10 μM) upon addition of various metal ions in HEPES buffer.

To ascertain the high selectivity of probe **3** for Al^{3+} ion interference studies have been performed in the presence of competitive metal ions particularly, Hg^{2+}, Cu^{2+}, Fe^{3+}, and Cr^{3+} . It is important to mention that upon addition of tested metal ions (in excess, 50 equiv.) to a solution of **3**+Al^{3+} or reversibly, addition of Al^{3+} (5 equiv) to

the solution of **3** containing other metal ions (**3**+M^{n+}; 50 equiv.) the relative fluorescence intensity and color of a probable complex, **3**+Al^{3+} remained unchanged except, a marginal interference of Fe^{3+} and Hg^{2+} ions in which relative fluorescence intensity quenched marginally (~5%) (Figure 2, bar diagram and S13). Thus, the experimental observation clearly favored the high sensitivity of **3** for Al^{3+} and the observed enhanced fluorescence is attributed to chelation-enhanced fluorescence effect (CHEF) as well as cation-induced inhibition of the ESIPT process due to the complexation of Al^{3+} with potential coordination sites present in probe **3** in the form aldimine (–HC=N) and hydroxy (–OH) functions.[4a,11,12,18] Additionally, the observed bright fluorescent color may also be attributed to the aggregation enhanced fluorescence which is very much possible in such kind of sytem.[18c]

The binding affinity of probe **3** with Al^{3+} has been realized through the absorption and emission titration studies (Figure 3a). Upon a gradual increase in the concentration of Al^{3+} ions (0-1.5 equiv) to a solution of **3** the absorption maxima centered, at 376 nm decreased and two new absorption bands appeared at 347 and 441 nm. The formation of two isosbestic point at 356 nm and 415 nm revealed the existence of more than one species in the medium. Similarly, the addition of Al^{3+} (0-1.5 equiv) to a solution of **3** the emission intensity centered, at 528 nm (λ_{ex}= 376 nm) enhanced, “turn-on” (about ~ 6 fold) significantly (Figure 3b) and the color of solution changed from a fluorescent dark green to a naked-eye sensitive bright yellow-green.

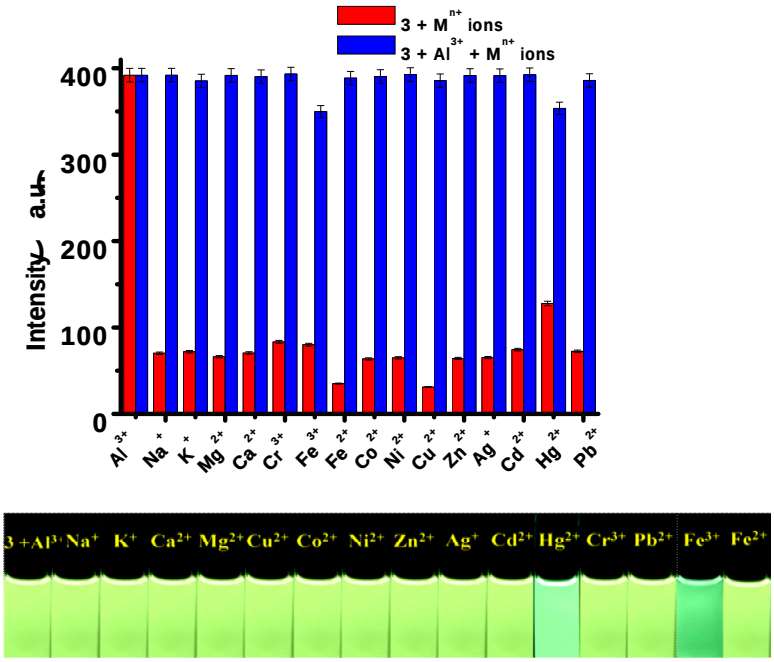

Figure 2: Bar diagram illustrate the change in emission intensity of **3** and a complex, **3+Al^{3+}** (10 μM) upon addition of tested metal ions in HEPES buffer (50%, H_2O/THF v/v, pH 7.04). Image: Change in color of a complex, **3+Al^{3+}** upon interference of tested metal ions under UV light at 365 nm.

To quantify the reaction stoichiometry between **3** and Al^{3+} absorption and emission spectra were acquired as a function of Al^{3+} ion concentration. Job's plot analysis revealed maxima at a mole fraction of 0.5 consistently. Thus, for a 1:1 stoichiometry between **3** and Al^{3+} the binding constants have been estimated through a nonlinear fittings of both absorption and emission spectra, using Benesi-Hildebrand (B-H) method[20] and were found to be K_{ass}(abs) = 7.8 x 10^5 /M and K_{ass}(em) = 8.46 x 10^5 /M, respectively (insets of Figure 3). Additionally, the molecular ion peak [**3** + Al + $3NO_3$ + MeOH + H]$^+$ appeared at *m/z* 753.7 in a positive ion ESI-MS spectrum confirmed the formation of a 1:1 complex, **3**+Al^{3+} (Figure S12).

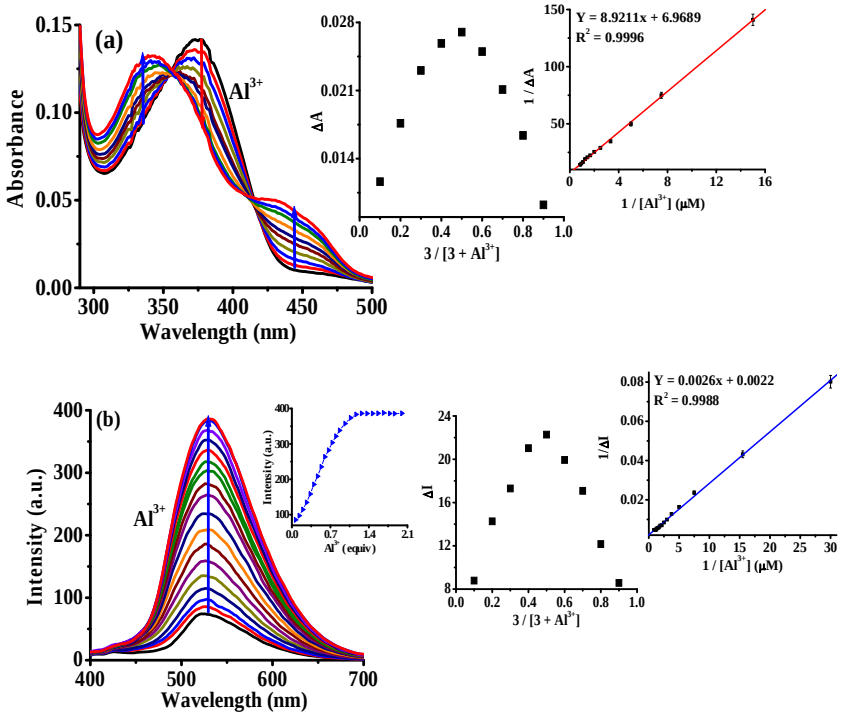

Figure 3: (a) Absorption and (b) emission titration spectra of **3** (10 μM) upon addition of 0-1.5 equiv of Al^{3+} ions in HEPES buffer (50% H_2O/THF v/v, pH 7.04). Insets: Job's plot and Benesi-Hildebrand plots.

2.2 Anion selectivity, reversibility and pH dependence of probe 3:

Additionally, to understand the high selectivity of **3** for Al^{3+} we also examined the photophysical behavior of **3** and its complex, **3**+Al^{3+} in the presence of different class of anions (F^-, Cl^-, Br^-, I^-, NO_3^-, N_3^-, SO_4^{2-},S^{2-}, $H_2PO_4^-$, CO_3^{2-}, AcO^-, and SCN^- (as their inorganic salts)) under the similar experimental condition in the HEPES buffer. It is important to mention that both the probe **3** and its complex, **3**+Al^{3+} have not shown any considerable affinity with anions as well as hindrance in the selective and sensitive detection of Al^{3+} (Figure S14).

Furthermore, to realize that the process of complexation between probe **3** and Al^{3+} is reversible a strong chelating agent, EDTA (25.0 equiv) was added to a solution of

probable complex, **3**+Al^{3+}. The fluorescence intensity revived and was found almost close to the intensity of **3** (Figure 4a). In contrast, when Al^{3+} ions were added to a solution of probe **3** containing EDTA (in excess) insignificant change was observed probably due to the formation of a strong EDTA-Al^{3+} complex (Figure 4b). These results thus, suggested about the reversible mode of complexation between **3** and Al^{3+} and can be potentially utilized to detect aluminium in a repeated cycle.

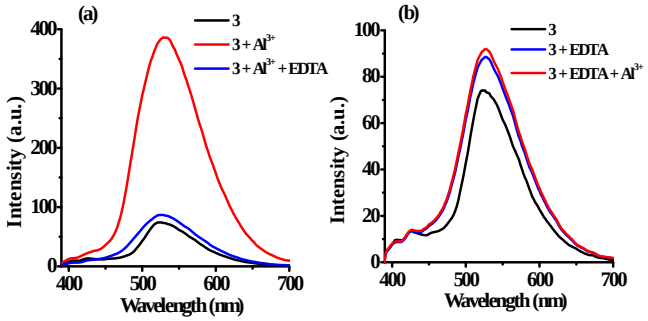

Figure 4: Change in emission spectra of **3** upon addition of (a) EDTA to a solution of **3** + Al^{3+} and (b) Al^{3+} ions to solution of **3**+EDTA in HEPES buffer (50% H_2O/THF v/v, pH 7.04).

The fluorescence behavior of probe **3** as a function of pH in the absence and presence of Al^{3+} has been examined in HEPES buffer (Figure 5). It is interesting to note that relative fluorescence intensity of **3** increases marginally (~1.5 fold) from pH 6 to 1 while considerable fluorescnec enhancement ocurs (~4 fold) under alkaline condition (pH 8 to 14), respectively. The observed relative emission intensity was high in alkaline medium and is attributed to deprotonation as well as existence of isomeric quinonoid form due to –C=N isomerization, while in acidic medium the observed increase in relative fluorescence intensity is attributed to protonation of either hydroxyl or amino function. In contrast, the emission behavior of a complex, **3**+Al^{3+} almost remained consistent in the pH range of 4 to 9 and beyond that could not sense Al^{3+} sensitively. We could reasoned this to either protonation of hydroxyl or

amino function or the decomposition of the **3**-Al^{3+} complex in acidic medium while the hydrolysis of Al^{3+} ion under the alkaline condition.[21] The other reason may be by the increase in pH the proton from the side functional groups remove and increase the extent of negative charges. Consequently, the highly charged functional groups repel each other as much as possible, causing the size of binding cavity to increase. When the cavity is stretched to a larger size, the binding force and interaction towards Al^{3+} ion are expected to decrease.[13] Thus, it is noteworthy to mention that probe **3** can work well at physiological pH (5 < pH < 7.5) and can be employed to detect Al^{3+} ions in pH range of 4-9 within which most of the biological and environment samples (5.25-8.93) can be also tested.[22]

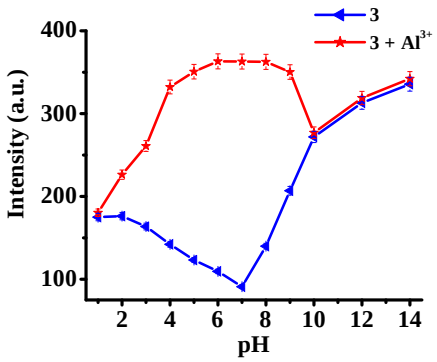

Figure 5: Change in emission intensity of **3** (10 μM, λ_{ex}=376 nm) at 528 nm in the absence and presence of 2.0 equiv of Al^{3+} as a function of pH in HEPES buffer (50% H_2O/THF v/v, pH 7.04).

2.3 Limit of Detection

The limit of detection (LOD) for Al^{3+} has been estimated through the fluorescence spectroscopic method, as reported previously.[15] A calibration curve was obtained by measuring the fluorescence spectra of probe **3** at different concentration (from 10 μM to 1.05 μM). An approximately straight calibration curve suggested about a linear

correlation between relative fluorescence intensities and concentrations of **3** along with standard deviation (σ) 0.5078 (Figure 6a). To estimate calibration sensitivity (m) fluorescence plots between ΔI ($I - I_0$) (where I_0 and I illustrate the emission intensities of **3** in the presence and absence of Al^{3+} ions) and concentration of Al^{3+} were obtained in the aforementioned range (Figure 6b). From the slope of fluorescence curve the calibration sensitivity (*m)* was found to be 68.5842 for which the limit of detection (LOD) has been estimated, employing equation (3), and was found to be 2.2 x 10^{-8} M (22 nM or ~0.6 ppb) which is comparable to other reported methods[11i-k, 14c,23, 24a-f] (Table -1) and well below the WHO acceptable limit (7.41 mM) in drinking water. Thus, the **3** can be applied to detect Al^{3+} in *nM* range which might fulfill the requirement of a potential fluorescent chemosensor to sense Al^{3+} in drinking water as well as in biosensing.

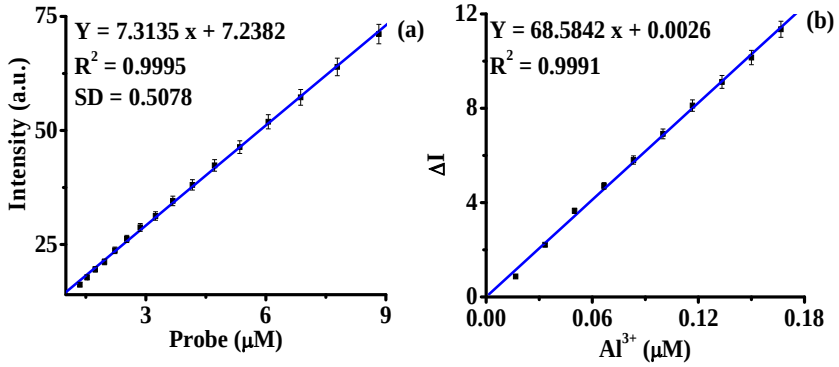

Figure 6: (a) Calibration curve for **3** (b) Calibration sensitivity curve (m) for **3** with Al^{3+} (where ΔI shows the change in emission intensity of **3** upon addition of Al^{3+}).

"Table 1"

Table 1: Comparison of some Schiff base chemosensors for Al^{3+} detection

Entry	Solvent system	LOD (M)	Quantum yield (Φ) (Probe to Probe+Al^{3+})	Binding Constant	References
1.	MeCN-H_2O (1:1, v/v)	0.42 x 10^{-6} M	-	7.0 x 10^3 M^{-1}	[14c]
2.	EtOH	10^{-7} M	-	1.24 x 10^7 M^{-1}	[24a]
3.	MeCN-H_2O HEPES Buffer (1:1, v/v)	3.24 x 10^{-8} M	0.01 to 0.42	-	[24b]
4.	MeCN-H_2O HEPES buffer (9:1, v/v)	6.03 x 10^{-6} M	-	5.02 x 10^4 M^{-1}	[24c]
5.	DMF-H_2O HEPES buffer (7:3, v/v)	5 x 10^{-6} M	-	5.1 x 10^3 M^{-1}	[24d]
6.	THF-H_2O HEPES buffer (7:1, v/v)	3 x 10^{-6} M	-	9.91 x 10^3 M^{-1}	[24e]
7.	EtOH-H_2O (95:5, v/v)	3.28 x 10^{-6} M	-	8.32 x 10^6 M^{-1}	[24f]
8.	MeOH	1.81 x 10^{-8} M	-	-	[11i]
9.	MeOH	4.79 x 10^{-8} M	-	1.41 x 10^4 M^{-1}	[11j]
10.	MeOH	8.28 x 10^{-8} M	-	1.59 x 10^4 M^{-1}	[11j]
11.	MeOH-DMSO (9:1, v/v)	6.0 x 10^{-7} M	< 0.001 to 0.11	5.7 x 10^3 M^{-1}	[11k]
12.	MeOH-DMSO (9:1, v/v)	5.8 x 10^{-7} M	< 0.001 to 0.059	1.6 x 10^4 M^{-1}	[11k]
13.	MeOH-DMSO (9:1, v/v)	5.0 x 10^{-7} M	< 0.001 to 0.054	1.9 x 10^3 M^{-1}	[11k]
14.	THF-H_2O HEPES buffer (1:1, v/v)	2.2 x 10^{-8} M	0.006 to 0.07	8.46 x 10^5 M^{-1}	Present work

2.4 Nature of Interaction between 3 and Al^{3+}

To have an insight about the mode of interaction between probe **3** and Al^{3+} the ^{1}HNMR titration experiments were performed in DMSO-d_6. The ^{1}H NMR spectrum of probe **3** (2.1×10^{-2} M) showed resonances corresponding to aromatic protons at δ 7.50 - 6.83 ppm (Figure – 7 and S7). The resonances appeared at δ 13.79, 9.71 and at δ 8.89 ppm are assignable to phenolic (–OH) H_b, H_a (disappeared completely upon D_2O treatment, Figure S8) and aldimine (–CH=N) protons, respectively. Upon a sequential addition of Al^{3+} ions (0-1.0 equiv) to a solution of probe **3**, the aldimine proton (CH=N-) was shifted downfield ($\Delta\delta$ = 0.012 ppm) with the subsequent splitting in the signal and appeared at δ 8.91 ppm. Moreover the phenolic protons H_b and H_a shifted downfield and become broadened while the aromatic protons exhibited upfield shift due to through bond charge propagation. Additionally, to understand the interaction of Al^{3+} ions with the phenolic and aldimine functions of **3** the FTIR spectra were acquired. The IR spectrum of **3** showed characteristic vibrations at 3430 cm^{-1} and at 1615 cm^{-1} attributable to stretching vibrations of -OH and aldimine functions (Figure S10, S16). Upon interaction of **3** with Al^{3+} the probable OH and C=N stretching vibrations shifted toward the lower frequency region and appeared at 3415 cm^{-1} and 1610 cm^{-1}, respectively (Figure S15, S16). These results altogether clearly suggested about the structural change ($E \rightarrow Z$) in the geometry of probe **3** as well as involvement of *O* (-OH, phenolic) and *N* (-CH=N, aldimine) atoms in the complexation with Al^{3+} ions as shown in Scheme 2.

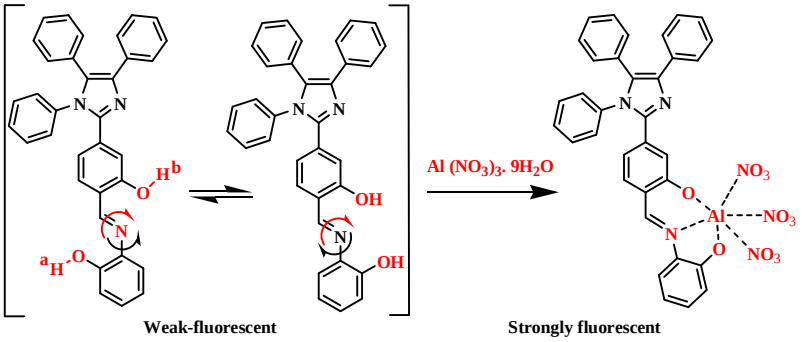

Scheme - 2: A plausible mode of binding between probe **3** and **Al^{3+}**.

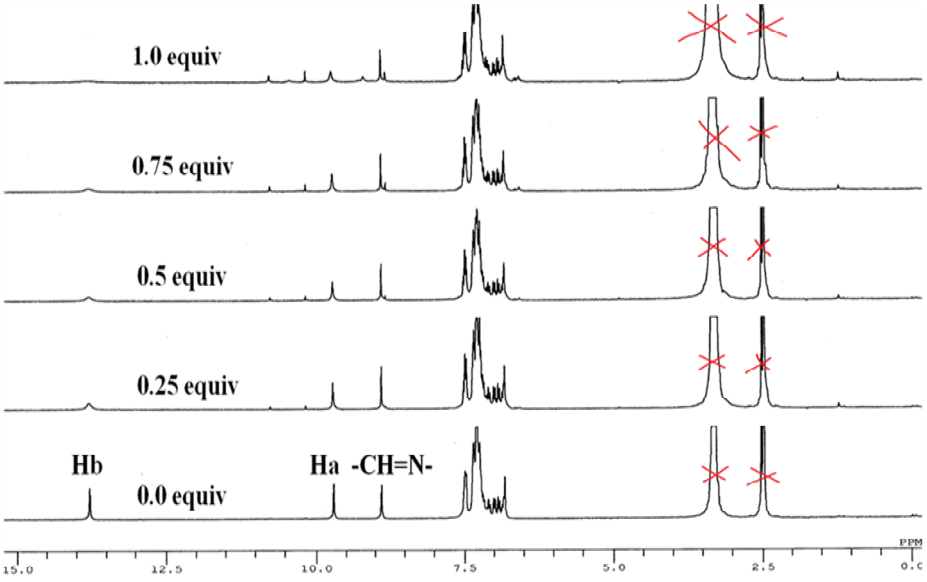

Figure 7: Stacked ^{1}H NMR spectra of **3** (2.1 x 10^{-2} M) upon addition of Al^{3+} (0-1.0 equiv) in DMSO-d_6.

3. Analytical application:

Detection of Al^{3+} in real contaminated water samples: To validate the practical analytical utility of probe **3** to determine concentration of Al^{3+} in real contaminated water samples, we first quantified the fluorescence of probe **3** (10 μM) in the presence of various concentration of Al^{3+} ion (0-0.2 μM) and the corresponding calibration plot was used as a standard curve (Figure 8a). Considering the possible interference of

other components present in real samples, we applied a standard addition method[15a] to determine the level of Al^{3+} in real water samples. Prior to real sample detection when probe **3** was added directly to the water samples, no significant fluorescence enhancement occurred. However, when the emission spectra of treated contaminated water samples were acquired, the recovery of Al^{3+} with respect to the standard calibration curve was excellent and we could quantify recovered Al^{3+} in real water samples within the range of 120 to 94% (Table 2), wherein the color of solution also changed from a weak fluorescent to a strong yellow-green that was readily visual to the naked-eye (Figure 8b).

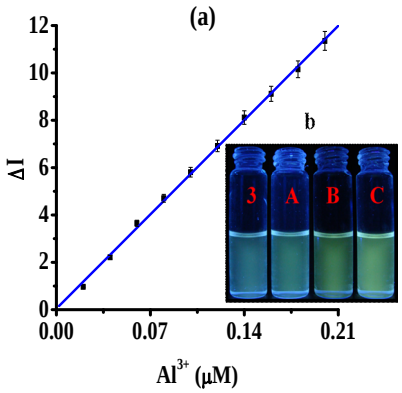

Figure 8: (a) Calibration sensitivity plot of **3** for Al^{3+} and (b) change in color of **3** and **3+** Al^{3+} solution (A = 0.002, B = 0.02, C = 0.2 μM) in HEPES buffer.

Table 2

Detection of Al^{3+} in real water samples

Sample concentration the sample	Al^{3+} recovered	% recovery of Al^{3+} from (μM)
0	Not detected	-
0.002	0.0024 ± 0.008	120
0.02	0.0194 ± 0.014	97
0.2	0.188 ± 0.025	94

***Detection of Al^{3+} on cellulose paper strip**:* In order to make sure the analytical use of probe **3**, on a solid surface, paper strip test was performed. Small cellulose paper strips (Whatman^{TM}) containing different concentration of probe **3** (1, 0.5, and 0.25 mM) were prepared (1.5 × 2.0 cm^2) in 50% aqueous THF and dried in air. The solution of of three different concentrations (5×10^{-6}, 5×10^{-7} and 5×10^{-8} M) of alumenium nitrate were prepared in water. The dried test paper strips were dipped in different concentration solutions of Al^{3+} for 10-15 min and dried in air. The observed color change of paper strips from fluorescent green to yellow under UV light at 365 nm (Figure-9) clearly, demonstrated the potential application of probe **3**. Further the test paper strip was capable to detect Al^{3+} ion up to 20 nM. Test paper strips of 0.1 and 0.01 mM concentration of probe were also made. The paper strip could able to detect Al^{3+} ions but the visibility of color on the strip was much better only up to 0.25 mM range.

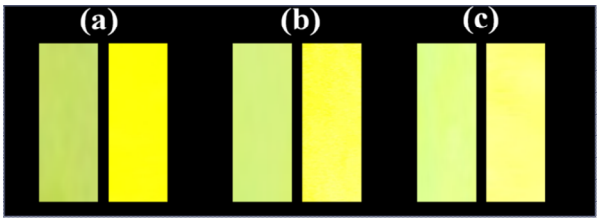

Figure 9: Fluorescent paper strips of 3 (a) 1 mM, (b) 0.5 mM, (c) 0.25 mM before (green) and after addition of Al^{3+} (a) 2 x 10^{-6}, (b) 2 x 10^{-7}, (c) 2 x 10^{-8} M (yellow).

4. Conclusion

In conclusion, we have developed a polynuclear hetero atom containing molecular organic scaffold that enabled Al^{3+} ion detection through fluorescence turn-on response in solution as well as on solid surface. The metal ion interaction studies in partial aqueous medium favors the complexation of Al^{3+} with *O* and *N* hetero atoms present

in the form of hydroxyl and aldimine functions of probe **3** through electrostatic interactions, and enabled chelation enhanced fluorescence in which the process of ESIPT and C=N isomerization became restricted. The probe has shown naked-eye sensitivity in which the color of solution turned on to a fluorescent yellow-green from a dark green color. We believe that the present findings have significance in the progress of Al^{3+} ion detection in the environment of competitive metal ions and anions.

Acknowledgment: The authors are thankful to the Council of Scientific and Industrial Research (CSIR), and the University Grant Commission (UGC) New Delhi for financial support and fellowships (to R.A., P.S, S.S.R) to carry out research work.

Supplementary data: General experimental details, synthesis and ^{1}H, ^{13}C NMR, FTIR, ESI-MS, HRMS spectroscopy data.

References

[1] (a) X. Chen, T. Pradhan, F. Wang, J. S. Kim and J. Yoon, *Chem. Rev.*, 2012, **112,** 1910-1956; (b) M. Shellaiah, Y.-H. Wu and H.-C. Lin, *Analyst*, 2013, **138,** 2931-2942; (c) V. Amendola, L. Fabbrizzi, F. Forti, M. Licchelli, C. Mangano, P. Pallavicini, A. Poggi, D. Sacchi and A. Taglieti, *Coord. Chem. Rev.,* 2006, **250,** 273-299; (d) J. Wu, W. Liu, J. Ge, H. Zhang and P. Wang, *Chem. Soc. Rev.*, 2011, **40**, 3483-3495; (e) S. Goswami, S. Paul and A. Manna, *RSC Adv.*, 2013, **3**, 25079-25085; (f) S. Goswami, K. Aich, S. Das, C. D. Mukhopadhyay, D. Sarkarc and T. K. Mondal, *Dalton Trans.*, 2015, **44**, 5763-5770.

[2] (a) A. P. de Silva, H. Q. N. Gunaratne, T. Gunnlaugsson, A. J. M. Huxley, C. P. McCoy, J. T. Rademacher, and T. E. Rice, *Chem. Rev.*, 1997, **97**, 1515-1566; (b) M. H. Lee, J. S Kim, and J. L. Sessler, *Chem. Soc. Rev.*, 2015, DOI: 10.1039/c4cs00280f.

[3] (a) D. T. Quang and J. S. Kim, *Chem. Rev.*, 2010, **110,** 6280-6301; (b) X. Chen, G. Zhou, X. Peng and J. Yoon, *Chem. Soc. Rev.*, 2012, **41,** 4610-4630; (c) T. Sakamoto, A. Ojida and I. Hamachi, *Chem. Commun.*, 2009, 141-152.

[4] (a) H. Xiao, K. Chen, N. Jiang, D. Cui, G.Yin, J. Wang and R. Wang, *Analyst*, 2014, **139**, 1980-1986; (b) X. B. Huang, Y. Dong, Q. W. Huang and Y. X. Cheng, *Tetrahedron Lett.*, 2013, **54**, 3822-3825; (c) Q. Y. Cao, Y. M. Han, H. M. Wang and Y. Xie, *Dyes Pigm.*, 2013, **99,** 798-802; (d) C. J. Gao, X. J. Jin, X. H. Yan, P. An, Y. Zhang, L. L. Liu, H. Tian, W. S. Liu, X. J. Yao and Y. Tang, *Sensors and Actuators B.*, 2013, **176**, 775-781.

[5] (a) C. Exley, *Environ. Sci.: Processes Impacts*, 2013, **15**, 1807-1816; (b) W. S. Miller, L. Zhuang, J. Bottema, A. J. Wittebrood, P. De Smet, A. Haszler and A. Vieregge, *Mater. Sci. Eng. A*, 2000, **280,** 37-49; (c) R. E. Doherty, *Environ. Forensics*, 2000, **1**, 83-93; (d) G. Ciardelli and N. Ranieri, *Water Res.*, 2001, **35**, 567-572.

[6] (a) G. Berthon, *Coord. Chem. Rev.*, 2002, **228,** 319-341; (b) M. I. Yousef, A. M. EI-Morsy and M. S. Hassan, *Toxicology*, 2005, **215**, 97-107; (c) J. L. Greger and J. E. Sutherland, *Crit. Rev. Clin. Lab. Sci.*, 1997, **34**, 439-474; (d) E. DeVoto and R. A. Yokel, *Environ. Health Perspect.*, 1994, **102**, 940-951; (e) T. Asada and H. Tamura, *J. Agric. Food Chem*., 2012, **42**, 10634-10640; (f) J.L. Greger, *Crit. Rev. Clin. Lab. Sci*., 1997, **5**, 439-474.

[7] C. Meriño-Gergichevich, M. Alberdi, A. G. Ivanov and M. Reyes-Díaz, *J. Plant Nutr. Soil Sci.*, 2010, **10**, 217-243; (b) M. L. Mora, M. A. Alfaro, S. C. Jarvis, R. Demanet and P. Cartes, *Soil Use Manage.*, 2006, **22**, 95-101.

[8] (a) J. R. Walton, *NeuroToxicology*, 2006, **27**, 385-394; (b) E. Altschuler, *Med. Hypotheses*, 1999, **53**, 22-23; (c) V. Frisardia, V. Solfrizzia, C. Capursob, P. G. Kehoec, B. P. Imbimbod, A. Santamatoe, F. Dellegraziea, D. Seripaf , A. Pilottof , A. Capursoa and F. Panzaa, *Journal of Alzheimer's Disease*, 2010, **20,** 17-30; (d) T. Han, X. Feng, B. Tong, J. Shi, L. Chen, J. Zhi and Y. Dong, *Chem. Commun*., 2012, **48**, 416-418; (e) G. D. Fasman, *Coord. Chem. Rev.*, 1996, **149**, 125-165; (f) S. H. Kim, H. S. Cho, J. Kim, S. J. Lee, D. T. Quang and J. S. Kim, *Org. Lett.*, 2010, **12,** 560-563;

(g) E. House, J. Collingwood, A. Khan, O. Korchazkina, G. Berthon and C. Exley, *Alzheimer's Dis.*, 2004, **6**, 291-301.

[9] WHO, Aluminium, Guidelines for Drinking-Water Quality, 4th ed., *World Health Organization*, Geneva, 2011.

[10] (a) Y. Zhao, Z. Lin, H. Liao, C. Duan and Q. Meng, *Inorg. Chem. Commun.*, 2006, **9**, 966-968; (b) L. Basabe-Desmonts, D. N. Reinhoudt and M. Crego-Calama, *Chem. Soc. Rev.*, 2007, **36**, 993-1017; (c) M. Zhang, Y. Q. Liu and B. C. Ye, *Chem.–Eur. J.*, 2012, **18**, 2507-2513; (d) X. Sun, Y. W. Wang and Y. Peng, *Org. Lett.*, 2012, **14**, 3420-3423.

[11] (a) A. Sahana, A. Banerjee, S. Lohar, B. Sarkar, S. K. Mukhopadhyay and D. Das, *Inorg. Chem.*, 2013, **52**, 3627-3633; (b) S. Guha, S. Lohar, A. Sahana, A. Banerjee, D. A. Safin, M. G. Babashkina, M. P. Mitoraj, M. Bolte, Y. Garcia, S. K. Mukhopadhyay and D. Das, *Dalton Trans.*, 2013, **42,** 10198-10207; (c) S. B. Maity and P. K. Bharadwaj, *Inorg. Chem.*, 2013, **52**, 1161-1163; (d) J. Y. Jung, S. J. Han, J. H. Chun, C. M. Lee and J. Yoon, *Dyes Pigm.*, 2012, **94,** 423-426; (e) L. Y. Wang, H. H. Li and D. R. Cao, *Sensors and Actuators B.*, 2013, **181**, 749-755; (f) T. H. Ma, M. Dong, Y. M. Dong, Y. W. Wang and Y. Peng, *Chem. Eur. J.*, 2010, **16**, 10313-10318; (g) S. Kim, J. Y. Noh, K. Y. Kim, J. H. Kim, H. K. Kang, S. W. Nam, S. H. Kim, S. Park, C. Kim and J. Kim, *Inorg. Chem.*, 2012, **51**, 3597-3602; (h) S. Sen, T. Mukherjee, B. Chattopadhyay, A. Moirangthem, A. Basu, J. Marek and P. Chattopadhyay, *Analyst*, 2012, **137**, 3975-3981; (i) V. K. Gupta, S. K. Shoora, L. K. Kumawat and A. K. Jain, *Sensors and Actuators B*, 2015, **209**, 15-24; (j) S. K. Shoora, A. K. Jain and V. K. Gupta, *Sensors and Actuators B*, 2015, **216**, 86-104; (k) N. Mergu, A. K. Singh and V. K. Gupta, *Sensors*, 2015, **15**, 9097-9111.

[12] (a) S. Sinha, R. R. Koner, S. Kumar, J. Mathew, P. V. Monisha, I. Kazia and S. Ghosh, RSC Adv., 2013, **3**, 345-351; (b) D. Maity and T. Govindaraju, *Inorg. Chem.*, 2010, **49,** 7229-7231; (c) C.-H. Chen, D.-J. Liao, C.-F. Wan and A.-T. Wu, *Analyst*, 2013, **138,** 2527-2530; (d) W.-H. Ding, W. Cao, X.-J. Zheng, D.-C. Fang, W.-T. Wong and L.-P. Jin, *Inorg. Chem.*, 2013, **52**, 7320-7322; (e) X. Shi, H. Wang, T. Han, X. Feng, B. Tong, J. Shi, J. Zhi and Y. Dong, *J. Mater. Chem.*, 2012, **22**, 19296-19302; (f) S. Samanta, B. Nath and J. B. Baruah, *Inorg. Chem. Commun*., 2012, **22**,

98-100; (g) Q. Meng, H. Liu, S. Cheng, C. Cao and J. Ren, *Talanta*, 2012, **99**, 464-470; (h) D. Maity and T. Govindaraju, *Chem. Commun*., 2012, **48**, 1039-1041; (i) W. Rodriguez-Cordoba, C. Fregoso, E. Zugazagoitia and J. Peon, *J. Phys. Chem. A*, 2007, **111,** 6241-6247; (j) K. Kaur, V. K. Bhardwaj, N. Kaur and N. Singh, *Inorganic Chemistry Communications*, 2012, **18**, 79-82; (k) V. K.Gupta, A. K. Jain and S. K. Shoora, *Sensors and Actuators B*, 2015, **219**, 218-231; (l) V.K. Gupta, N. Mergu, L. K. Kumawat and A. K. Singh, *Talanta*, 2015, **144**, 80-89.

[13] (a) S. M. Ng and R. Narayanaswamy, *Anal Bioanal Chem*, 2006, **386**, 1235-1244; (b) J. L. Ren, J. Zhang, J. Q. Luo, X. K. Pei, and Z. X. Jiang, *Analyst*, 2001, **126**, 698-702; (c) V.K. Gupta, A.K. Singh and L.K. Kumawat, *Sensors and Actuators B.*, 2014, **195**, 98-108; (d) V.K. Gupta, A.K. Singh and N. Mergu, *Electrochim. Acta*, 2014, **117**, 405-412.

[14] (a) B. Ramachandram and A. Samanta, *Chem. Commun.*, 1997, 1037-1038; (b) U. Fegade, S. Attarde and A. Kuwar, *Chem. Phys. Lett.*, 2013, **584**, 165-171; (c) R. Patil, A. Moirangthem, R. Butcher, N. Singh, A. Basu, K. Tayade, U. Fegade, D. Hundiwale and A. Kuwar, *Dalton Trans.*, 2014, **43**, 2895-2899.

[15] (a) P. Srivastava, S. S. Razi, R. Ali, R. C. Gupta, S. S. Yadav, G. Narayan and A. Misra, *Anal. Chem.*, 2014, **86**, 8693-8699; (b) A. Misra, P. Srivastava and M. Shahid, *Analyst*, 2012, **137,** 3470-3478; (c) P. Srivastava, M. Shahid and A. Misra, *Org. Biomol. Chem.*, 2011, **9,** 5051-5055; (d) P. Srivastava, R. Ali, S. S. Razi, M. Shahid and A. Misra, *Sensors and Actuators B.*, 2013, **181,** 584-595; (e) A. Misra, M. Shahid and P. Srivastava, *Sensors and Actuators B*., 2012, **169,** 327-340; (f) P. Srivastava, R. Ali, S. S. Razi, M. Shahid, and A. Misra, *Sensors and Actuators B*., 2013, **181,** 584-595**;** (g) P. Srivastava, R. Ali, S. S. Razi, M. Shahid, S. Patnaik and A. Misra, *Tetrahedron Lett.*, 2013, **54,** 3688-3693; (h) S. S. Razi, P. Srivastava, R. Ali, R. C. Gupta, S. K. Dwivedi and A. Misra, *Sensors and Actuators B.*, 2015, **209,** 162-171.

[16] (a) D. M. D'Souza, A. Kiel, D. P. Herten, F. Rominger and T. J. J. Muller, *Chem. Eur. J.*, 2008, **14,** 529-547; (b) J. E. Biggs-Houck, A. Younai and J. T. Shaw, *Current Opinion in Chemical Biology*, 2010, **14**, 371-382; (c) B. B. Toure and D. G. Hall, *Chem. Rev.*, 2009, **109**, 4439-4486; (d) K. Ramesh, S. N. Murthy, K. Karnakar, Y.V.D. Nageswar, K. Vijayalakhshmi, B. L. A. P. Devi and R. B. N. Prasad,

Tetrahedron Letters, 2012, **53**, 1126-1129; (e) S. D. Sharma, P. Hazarika and D. Konwar, *Tetrahedron Letters*, 2008, **49**, 2216-2220.

[17] (a) S. Park, O-H. Kwon, S. Kim, S. Park, M-G. Choi, M. Cha, S. Y. Park and D-J. Jang, *J. Am. Chem. Soc.*, 2005, **127,** 10070-10074; (b) B. S. Furniss, A. J. Hannaford, P. W. G. Smith and A. R. Tatchell, "Vogel's Textbook of Practical Organic Chemistry" , 5th edition, 2006.

[18] (a) T. Han, X. Feng, B. Tong, J. Shi, L. Chen, J. Zhic and Y. Dong, *Chem. Commun.*, 2012, **48**, 416-418; (b) B. Valeur and I. Leray, *Coord. Chem. Rev.*, 2000, **205**, 3-40; (c) Y. Hong, J. W. Y. Lama and B. Z. Tang, *Chem. Soc. Rev.*, 2011, **40**, 5361-5388.

[19] J. R. Lakowicz, ''*Principles of Fluorescence Spectroscopy*'', 3rd edition, Springer, New York 2006.

[20] H. A. Benesi and J. H. Hildebrand, *J. Am. Chem. Soc*., 1949, **71**, 2703-2707.

[21] (a) K. Hellgardt and D. Chadwick, *Ind. Eng. Chem. Res.*, 1998, **37,** 405-411; (b) M. Druchok, M. Holovko and T. Bryk, *Condensed Matter Physics*, 2004, **7,** 699-707.

[22] P. Srivastava, S. S. Razi, R. Ali, S. Srivastav, S. Patnaik, S. Srikrishna and A. Misra, *Biosensors and Bioelectronics*, 2015, **69**, 179-185.

[23] L. Elečková, M. Alexovič, J. Kuchár, I. S. Balogh and V. Andruch, *Talanta*, 2015, **133**, 27-33.

[24] (a) Z.-C. Liao, Z.-Y. Yang, Y. Li, B.-D. Wang and Q.-X. Zhou, *Dyes and Pigments*, 2013, **97**, 124-128; (b) S. Goswami, K. Aich, S. Das, A. K. Das, D. Sarkar, S. Panja, T. K. Mondal and S. Mukhopadhyay, *Chem. Commun*., 2013, **49**, 10739-10741; (c) Y. J. Lee, C. Lim, H. Suh, E. J. Song and C. Kim, *Sensors and Actuators B*, 2014, **201**, 535-544. (d) K. Kaur, V. K. Bhardwaj, N. Kaur and N. Singh, *Inorganic Chemistry Communications*, 2012, **18**, 79-82; (e) K. Kaur, V. K. Bhardwaj, N. Kaur and N. Singh, *Inorganic Chemistry Communications*, 2012, **26**, 31-36; (f) Y.-W. Liu, C.-H. Chen and A.-T. Wu, *Analyst*, 2012, **137**, 5201-5203.

Figure Captions

Scheme 1. Synthesis of probe **3**

Figure 1: (a) Absorption and (b) emission spectra of **3** (10 μM) upon interaction with different metal ions (2.0 equiv) in HEPES buffer (50% H_2O/THF v/v, pH 7.04). **Images**: Chromogenic and fluorogenic (under UV light at 365 nm) response of **3** (10 μM) upon addition of various metal ions in HEPES buffer.

Figure 2: Bar diagram illustrate the change in emission intensity of **3** and a complex, **3+Al^{3+}** (10 μM) upon addition of tested metal ions in HEPES buffer (50%, H_2O/THF v/v, pH 7.04). Image: Change in color of a complex, **3+Al^{3+}** upon interference of tested metal ions under UV light at 365 nm.

Figure 3: (a) Absorption and (b) emission titration spectra of **3** (10 μM) upon addition of 0-1.5 equiv of Al^{3+} ions in HEPES buffer (50% H_2O/THF v/v, pH 7.04). Insets: Job's plot and Benesi-Hildebrand plots.

Figure 4: Change in emission spectra of **3** upon addition of (a) EDTA to a solution of **3** + Al^{3+} and (b) Al^{3+} ions to solution of **3**+EDTA in HEPES buffer (50% H_2O/THF v/v, pH 7.04).

Figure 5: Change in emission intensity of **3** (10 μM, λ_{ex}=376 nm) at 528 nm in the absence and presence of 2.0 equiv of Al^{3+} as a function of pH in HEPES buffer (50% H_2O/THF v/v, pH 7.04).

Figure 6: (a) Calibration curve for **3** (b) Calibration sensitivity curve (m) for **3** with Al^{3+} (where ΔI shows the change in emission intensity of **3** upon addition of Al^{3+}).

Figure 7: Stacked ^1H NMR spectra of **3** (2.1 x 10^{-2} M) upon addition of Al^{3+} (0-1.0 equiv) in DMSO-d_6.

Scheme - 2: A plausible mode of binding between probe **3** and **Al^{3+}**.

Figure 8: (a) Calibration sensitivity plot of **3** for Al^{3+} and (b) change in color of **3** and **3+** Al^{3+} solution (A = 0.002, B = 0.02, C = 0.2 μM) in HEPES buffer.

Table 1: Comparison of some Schiff base chemosensors for Al^{3+} detection.

Table 2: Detection of Al^{3+} in real water samples.

Figure 9: Fluorescent paper strips of 3 (a) 1 mM, (b) 0.5 mM, (c) 0.25 mM before (green) and after addition of Al^{3+} (a) 2 x 10^{-6}, (b) 2 x 10^{-7}, (c) 2 x 10^{-8} M (yellow).

SUPPLEMENTARY INFORMATION

A polynuclear hetero atom containing molecular organic scaffold to detect Al^{3+} ion through fluorescence Turn-On response

Rashid Ali, Syed S. Razi, Priyanka Srivastava, Mohammad Shahid, and Arvind Misra*

Department of Chemistry, Faculty of Science, Banaras Hindu University, Varanasi – 221 005 UP INDIA

Corresponding author e-mail: arvindmisra2003@yahoo.com; amisra@bhu.ac.in

Contents

Figure S13: (a) Absorption and (b) emission spectra of interference studies upon addition of tested metal ions to a solution of **3**+Al^{3+} (10 μM) in HEPES buffer (v/v = 50%, pH 7.04).

Figure S14: (a) Emission and Absorption (inset) spectra of **3** (10 μM) upon interaction of various anions (50.0 equiv) in HEPES buffer (v/v = 50%, pH 7.04). (b) Emission spectra of interference studies upon addition of different anions to a solution of **3**+Al^{3+} (10 μM) in HEPES buffer (v/v = 50%, pH 7.04).

Figure S15: FT-IR spectrum of **3+Al^{3+}** complex.

Figure S16: Stacked FT-IR spectrum of **3** and **3+Al^{3+}** complex.

Table S1: Photophysical properties of probe **3** and **3+Al^{3+}** in different solvents and water gradient systems

Experimental

General: All the reagents and solvents were purchased from Sigma-Aldrich Chemical Co. Pvt. Ltd. stored in a desiccator under vacuum containing self indicating silica, and used without any further purification. Solvents were purified prior to use. UV-vis absorption spectra were recorded on a Perkin Elmer Lambda-35 UV-vis spectrophotometer using a quartz cuvette (path length = 1cm). Infrared (IR) spectra were recorded in potassium bromide (KBr) on a FT-IR Perkin Elmer Spectrophotometer. ^{1}H NMR spectra (chemical shifts in δ ppm) were recorded on a JEOL AL 300 FT-NMR (300 MHz) spectrometer, using tetramethylsilane (TMS) as internal standard. Fluorescence spectra were recorded on Varian eclipse Carry spectrofluorometer using a quartz cuvette (path length = 1 cm) at 600 PMT voltage and slit width 5nm/5nm. All the spectroscopic experiments were carried out at room temperature. The stock solution of **3** ($1x10^{-3}$ M) were prepared in THF and diluted to obtain 10 μM solution in THF/HEPES buffer (v/v = 50%, pH 7.0) for the absorption and fluorescence measurements, respectively. The stock solutions of different metal ions ($1x10^{-1}$ M) were prepared by dissolving their nitrate salt in water. The cation interaction studies were performed by the addition of 2 equiv. of $1x10^{-1}$ M of different cations. The absorption and fluorescence titration experiment were performed by the gradual increase of concentration of Al^{3+} (c =$1x10^{-3}$). The cation interference studies were performed by the addition of 50 equiv. of $1x10^{-1}$ M of different cations. For ^{1}H NMR titration experiment solution of probe **3** ($1x10^{-2}$ M) and $Al(NO_3)_3$ was prepared in DMSO-d_6.

The quantum yields were estimated with respect to the quinine sulfate as standard in 0.1M H_2SO_4 solution by secondary methods, [19] using equation (1).

$$Q = Q_R . I/I_R . OD_R/OD . n^2/n^2_R \quad (1)$$

Where Q is the quantum yield, *I* is the integrated intensity, OD is the optical density, and n is the refractive index. The subscript R refers to the reference fluorophore of known quantum yield.

The absorption and fluorescence experimental data were utilized to calculate association constants by Benesi-Hildebrand method [20] (B-H method) employing equations (1) for 1:1 stoichiometries.

$$1/(I - I_o) = 1/(I - I_f) + 1/K(I - I_f)[M] \quad (2)$$

Where K is the association constant, I is the absorbance/fluorescence intensity of the free probe **3**, I_o is the observed absorbance/fluorescence intensity of the **3-Al^{3+}** complex, and I_f is the absorbance/fluorescence intensity at saturation level.

The limit of detection (LOD) was estimated by using equation (3).

$$LOD = 3\sigma / m \quad (3)$$

Where, σ stands for the standard deviation of blank solution of **3** and m stands for calibration sensitivity toward Al^{3+} in THF/HEPES buffer (v/v = 50%, pH 7.04) solution.

Synthesis of compound 1: Benzil (1.05 g, 5 mmol) and *m*-hydroxybenzaldehyde (610 mg, 5 mmol) were dissolved in glacial acetic acid (20 mL) at room temperature. To this solution aniline (0.7 mL, 7.5 mmol) was added dropwise. After the addition of ammonium acetate (2.0 g, 26 mmol) the reaction mixture was heated at 110 ^{0}C for 4 hr and monitored the reaction on TLC. After completion of reaction, the reaction mixture was cooled to room temperature and poured into the ice-water. The precipitate was filtered, washed with cold water, air dried and recrystallized from ethylacetate to get compound **1** as a light brown color powder. Yield 1.4 g (72%). R_f = 0.52 (Ethylacetate:DCM:: 2:8, v/v). ^{1}H NMR (300 MHz, DMSO-d_6)**:** δ (ppm): 9.52 (s, 1H, -OH), 7.48-7.62 (d, 2H, J = 7.2 Hz), 7.31-7.16 (m, 13H), 7.04-6.99 (t, 1H, J_1 = 7.8 Hz, J_2 =7.8 Hz), 6.94 (s, 1H); 6.67 (m, 2H). FT-IR (KBr) ν_{max} (cm^{-1}); 3051, 1597, 1582, 1497,1482, 1443, 1397, 1376, 1300, 1213, 1178, 1076, 998, 970, 884, 766, 695.

Synthesis of compound 2: Compound **2** was synthesized by formylation of compound **1** using Reimer-Tiemann reaction. Compound **1** (1.4 g, 3.65 mmol) was taken in dry ethanol (6 mL) and an aqueous solution (15 mL) of KOH (0.9 g, 16 mmol) was added. The reaction mixture was heated at 70-80^{0}C and then added $CHCl_3$ (1.43 g, 0.97 mL, 12 mmol) dropwise for 10-20 min. Once the color of reaction mixture became brine red stirring was continued for 2hr and then at room temperature for 2-3hr. The excess of $CHCl_3$ and EtOH were distilled off and the residue was treated with conc. HCl to make the pH of solution acidic (pH 2-3). After the addition of water (15 mL) precipitate was filtered, washed with water, air dried and purified by coloumn chromatography using dichloromethane as eluent. The solvent was evaporated in vacuum to get compound **2.** Yield=100 mg (7%). R_f = 0.56 (Ethylacetate:DCM:: 0.5:9.5, v/v), ^{1}H NMR (300 MHz, DMSO-d_6)**:** δ (ppm); 10.76 (s, 1H, -OH), 10.19 (s, 1H, -CHO), 7.49-7.47 (d, 2H, J = 6.3 Hz), 7.35-7.15 (m, 16H). ^{13}C NMR (75 MHz, DMSO-d_6)**:** δ (ppm); 190.89, 160.19, 144.60, 137.44, 137.27, 136.33, 134.06, 132.34, 131.09, 130.01, 129.30, 129, 128.80, 128.54, 128.21, 126.68, 126.38, 121.65, 118.99, 116.68. FT-IR (KBr) ν_{max} (cm^{-1}); 3415, 3051, 2962, 2924, 2850,1662, 1626, 1595,1495, 1461, 1381, 1315, 1261, 1204, 1097, 1025, 966, 914, 874, 805, 701. HRMS (micrOTOF-Q) m/z: [PHA + H]$^+$ calc. for C28H20N2O2, 417.1598; Found 417.1598.

Synthesis of compound 3: Compound **2** (100 mg, 0.24 mmol) and 2-aminophenol (27 mg, 0.24 mmol) were taken in acetonitrile (10 mL) and stirred at room temperature for 15 min to get a clear solution. The reaction mixture was refluxed for 2 hr in the presence of iodine (3 mol % of reactant). The red colored precipitate so obtained was filtered, washed with acetonitrile and dried in air to get the desired

compound **3** in good yield 90% (110 mg). R_f = 0.62 (Ethylacetate:DCM:: 0.5:9.5, v/v), ^{1}H NMR (300 MHz, DMSO-d_6) δ (ppm): 13.79 (1H, -OH, H_b), 9.71 (1H, -OH, H_a), 8.89 (s, 1H, -HC=N), 7.50-7.47 (d, 2H, *J* = 6.3Hz), 7.35-7.08 (m, 17H), 7.02-6.99 (d, 1H, *J* = 7.8 Hz), 6.94-6.92 (d, 1H, *J* = 7.8 Hz), 6.85-6.83 (d, 1H, *J* = 6.3 Hz). ^{13}C NMR (75 MHz, DMSO-d_6) δ (ppm): 160.75, 151.30, 145.25, 137.44, 136.71, 134.76, 134.28, 134.09, 132.22, 132.10, 131.30, 130.26, 129.48, 129.20, 128.68, 128.42, 126.92, 126.62, 119.87, 119.26, 118.77, 116.69, 116.27. FT-IR (KBr) ν_{max} (cm^{-1}); 3430, 3061, 2958, 2924, 2852, 1615, 1515, 1506, 1497, 1465, 1352, 1285, 1224, 1163, 1119, 925, 722, 694. HRMS (microTOF-Q) m/z: $[3 + H]^+$ calc. for C34H25N3O2, 508.2019; Found 508.2019.

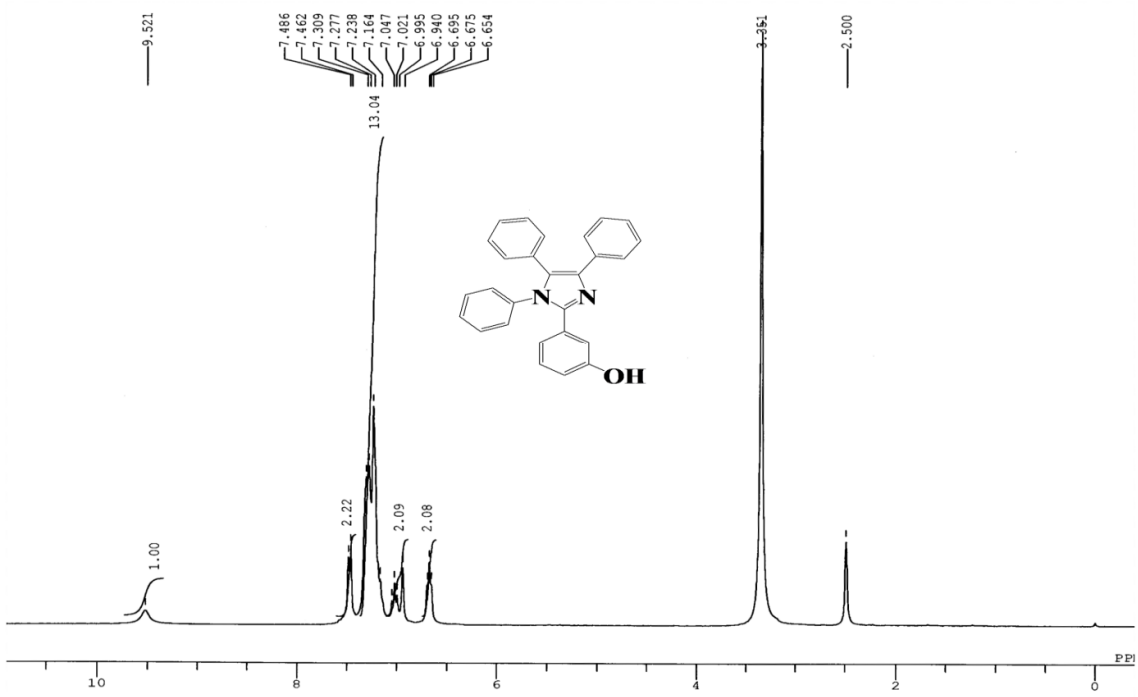

Figure S1: ^{1}H NMR spectrum of **1** in DMSO-d_6.

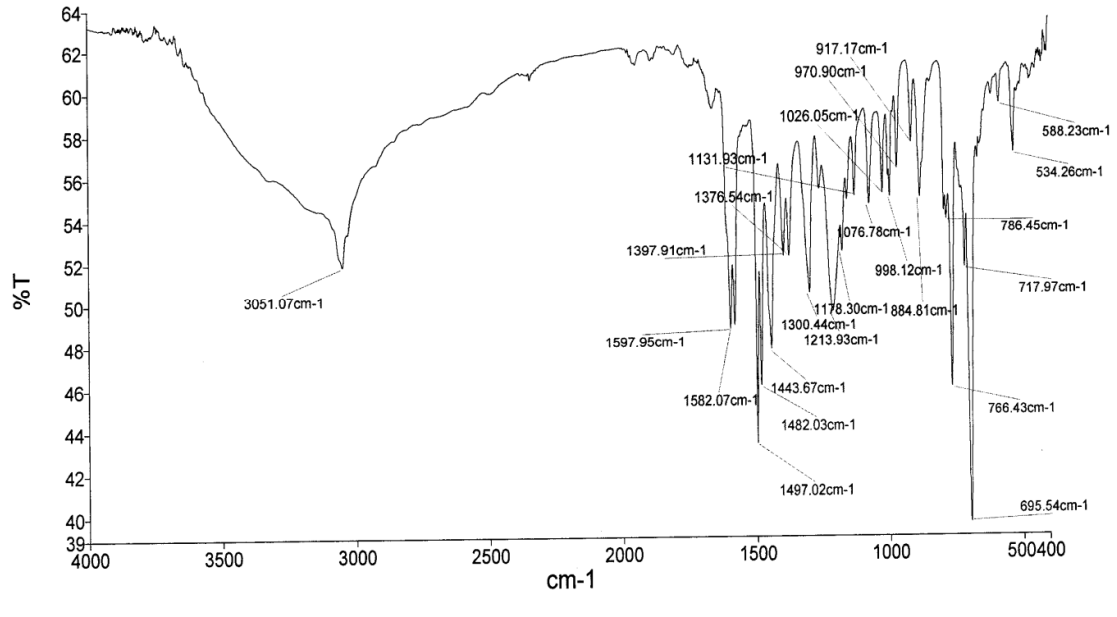

Figure S2: FT-IR spectrum of **1**.

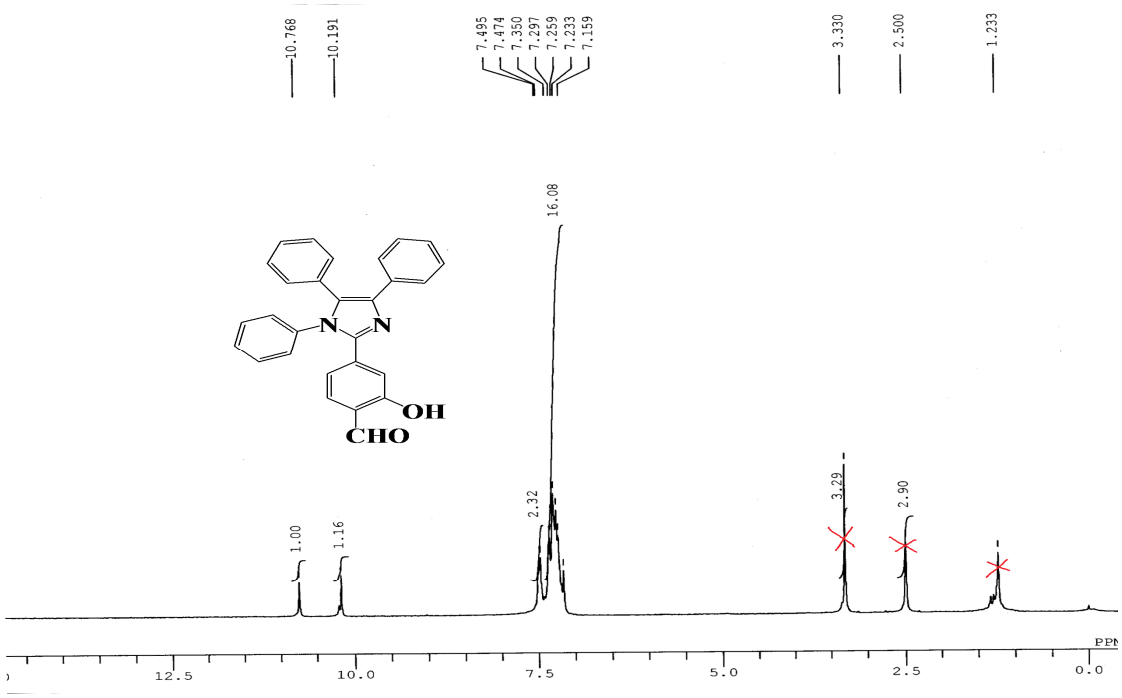

Figure S3: ^{1}H NMR spectrum of **2** in DMSO-d_6.

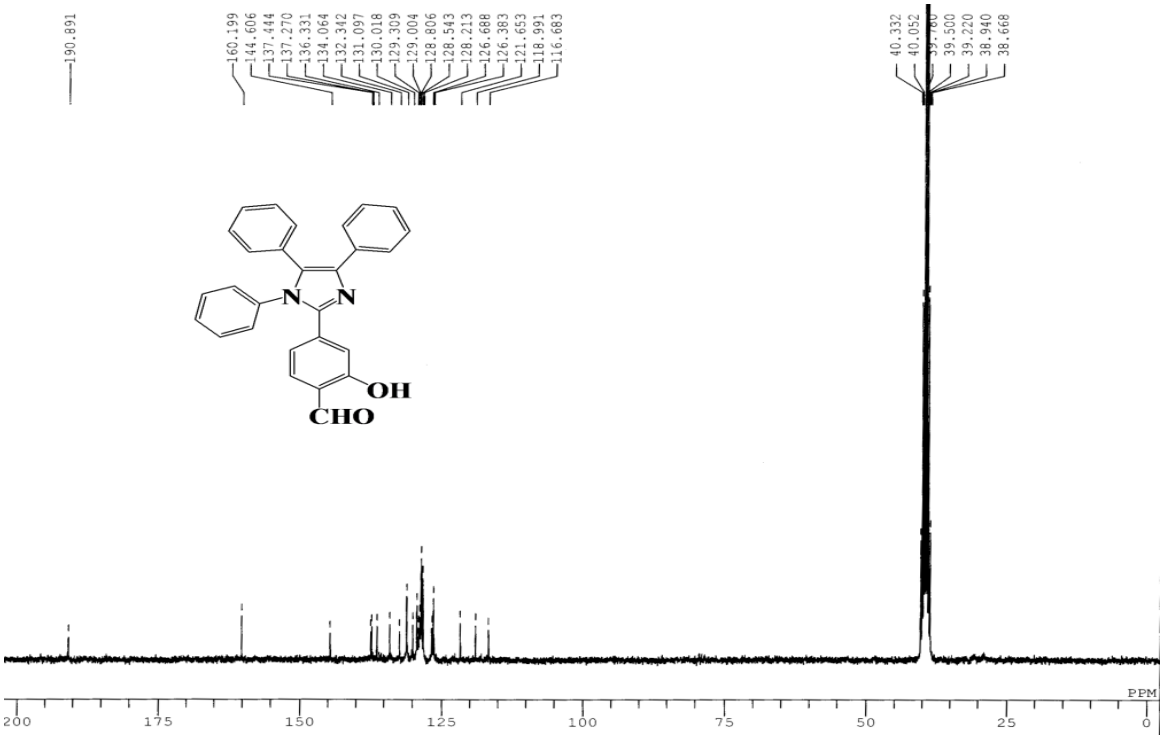

Figure S4: ^{13}C NMR spectrum of **2** in DMSO-d_6.

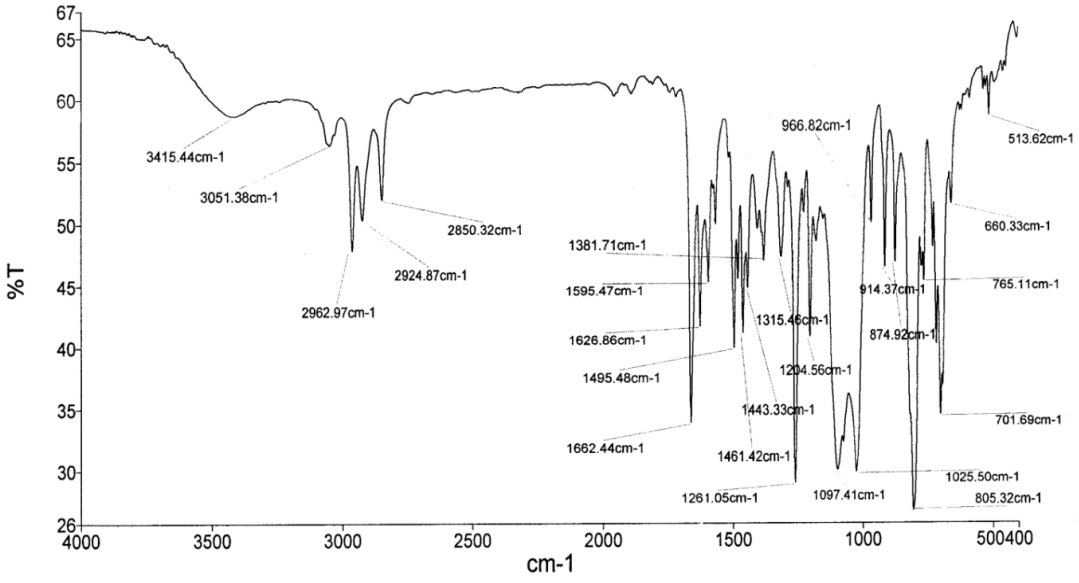

Figure S5: FT-IR spectrum of **2**.

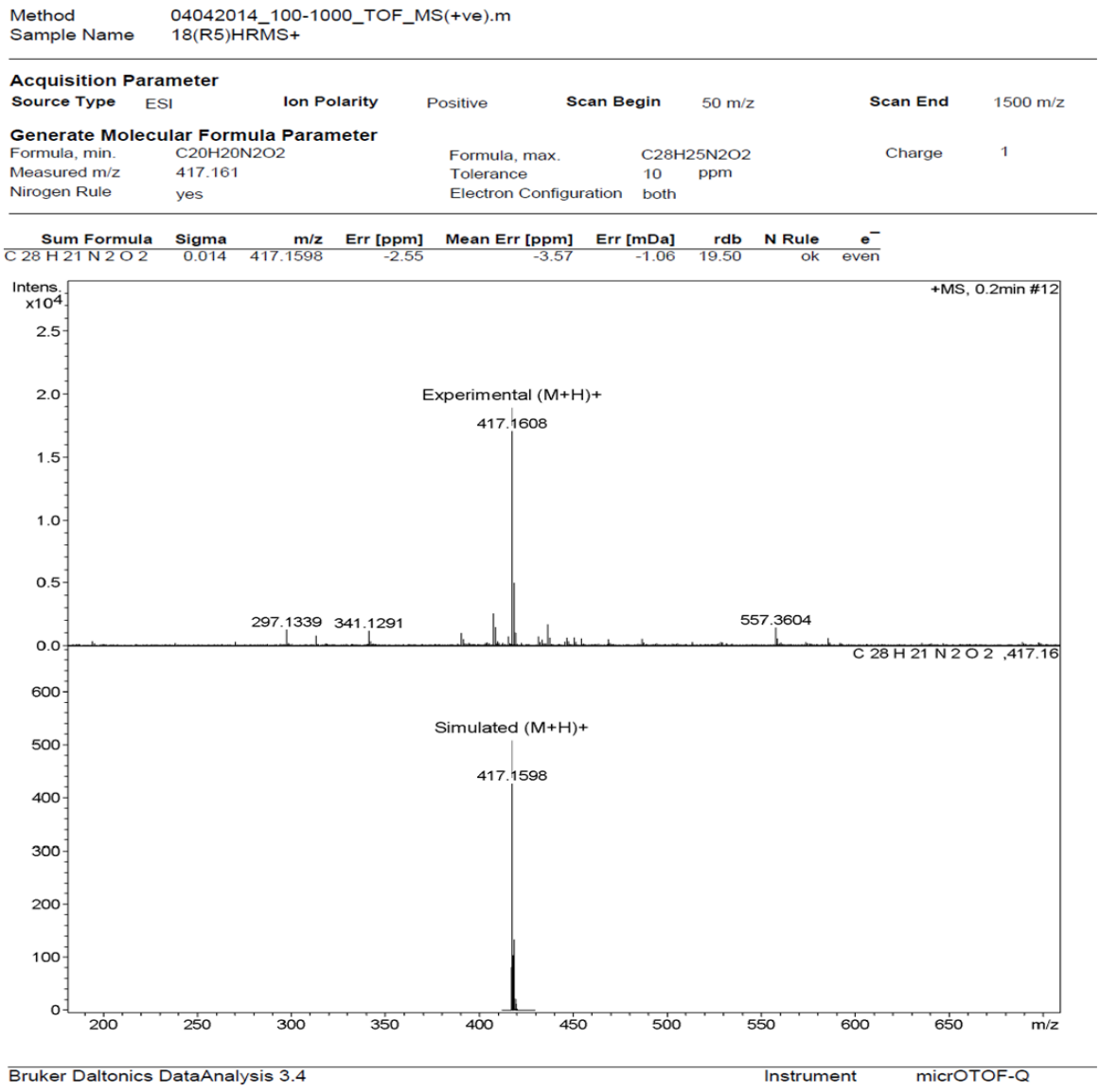

Figure S6: HRMS spectrum of **2.**

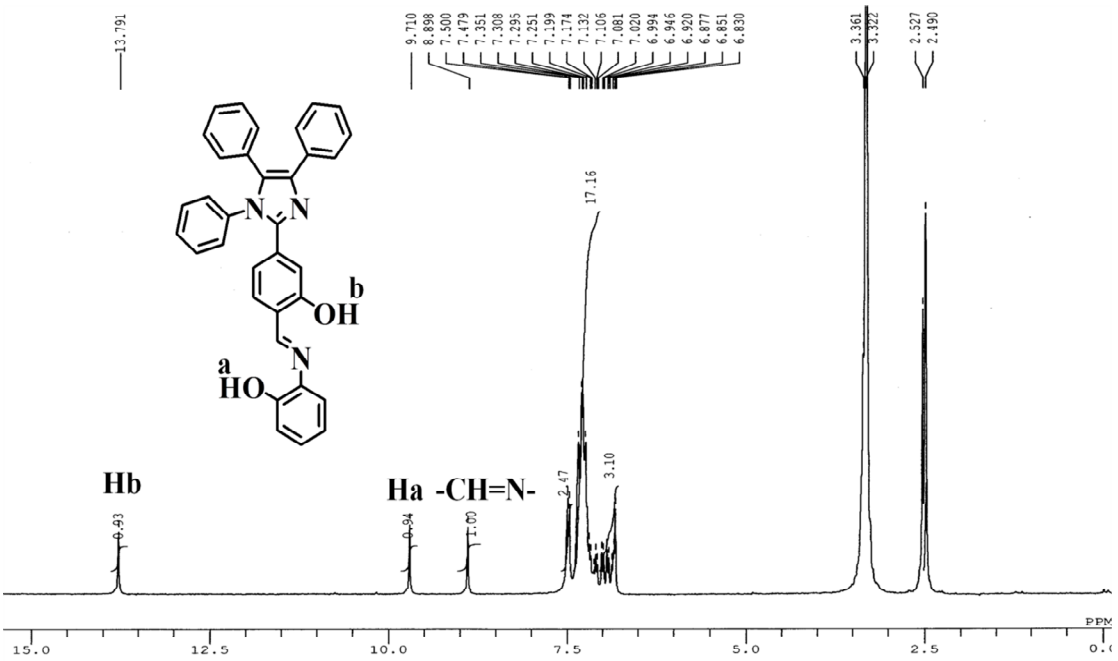

Figure S7: ^{1}H NMR spectrum of **3** in DMSO-d_6.

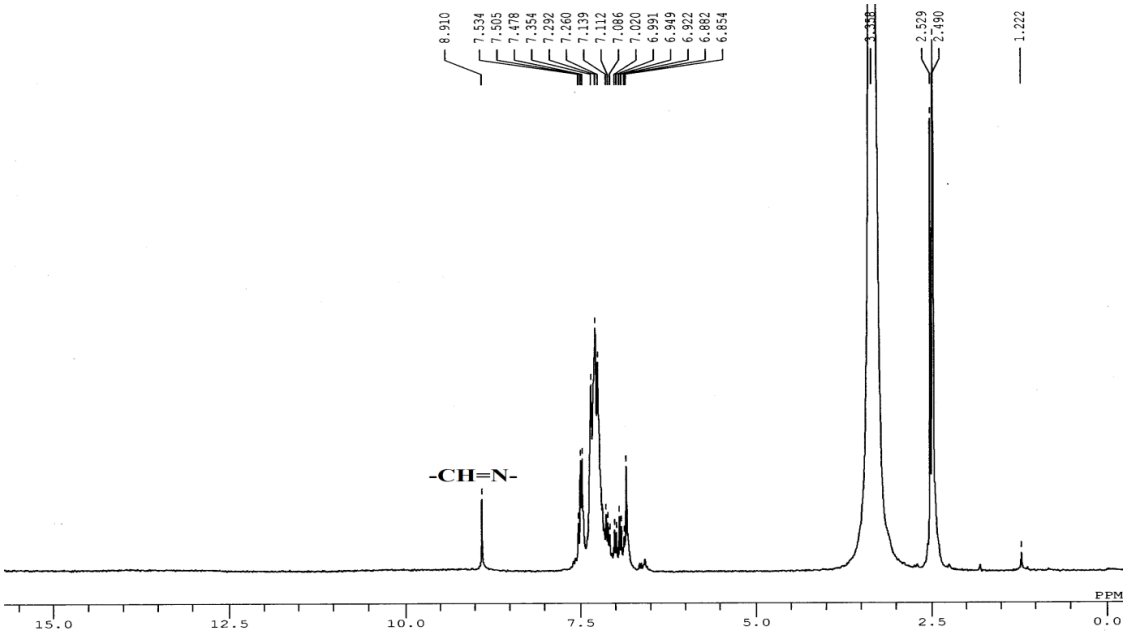

Figure S8: D_2O exchange ^{1}H NMR spectrum of **3** in DMSO-D_2O (9:1).

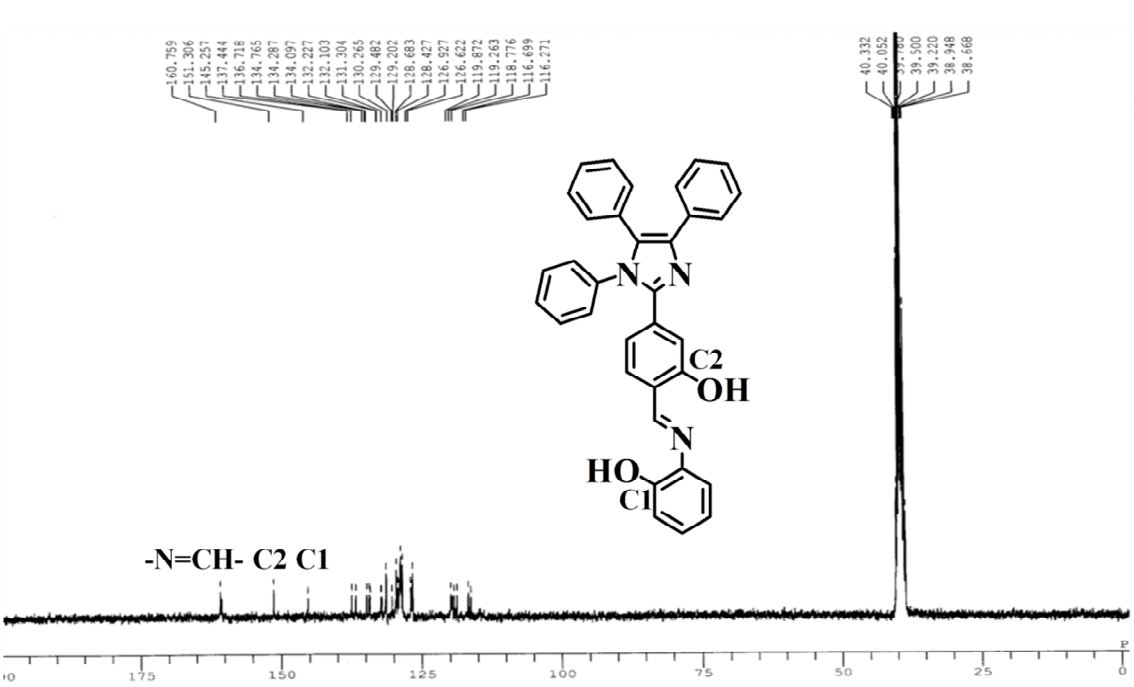

Figure S9: ^{13}C NMR spectrum of **3** in DMSO-d_6.

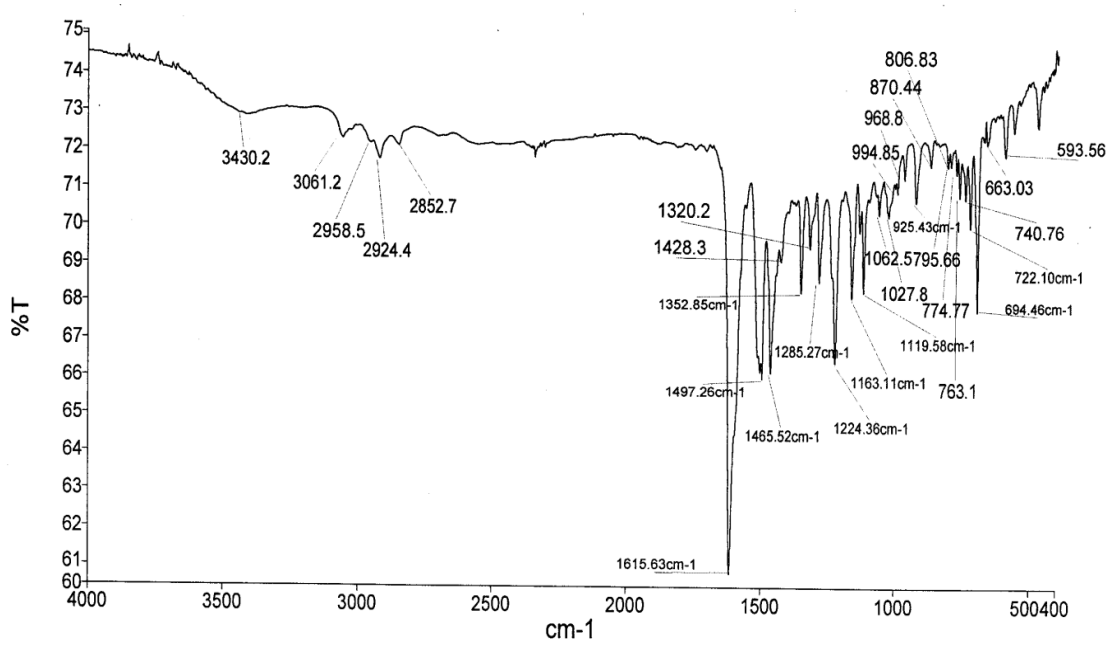

Figure S10: FT-IR spectrum of **3.**

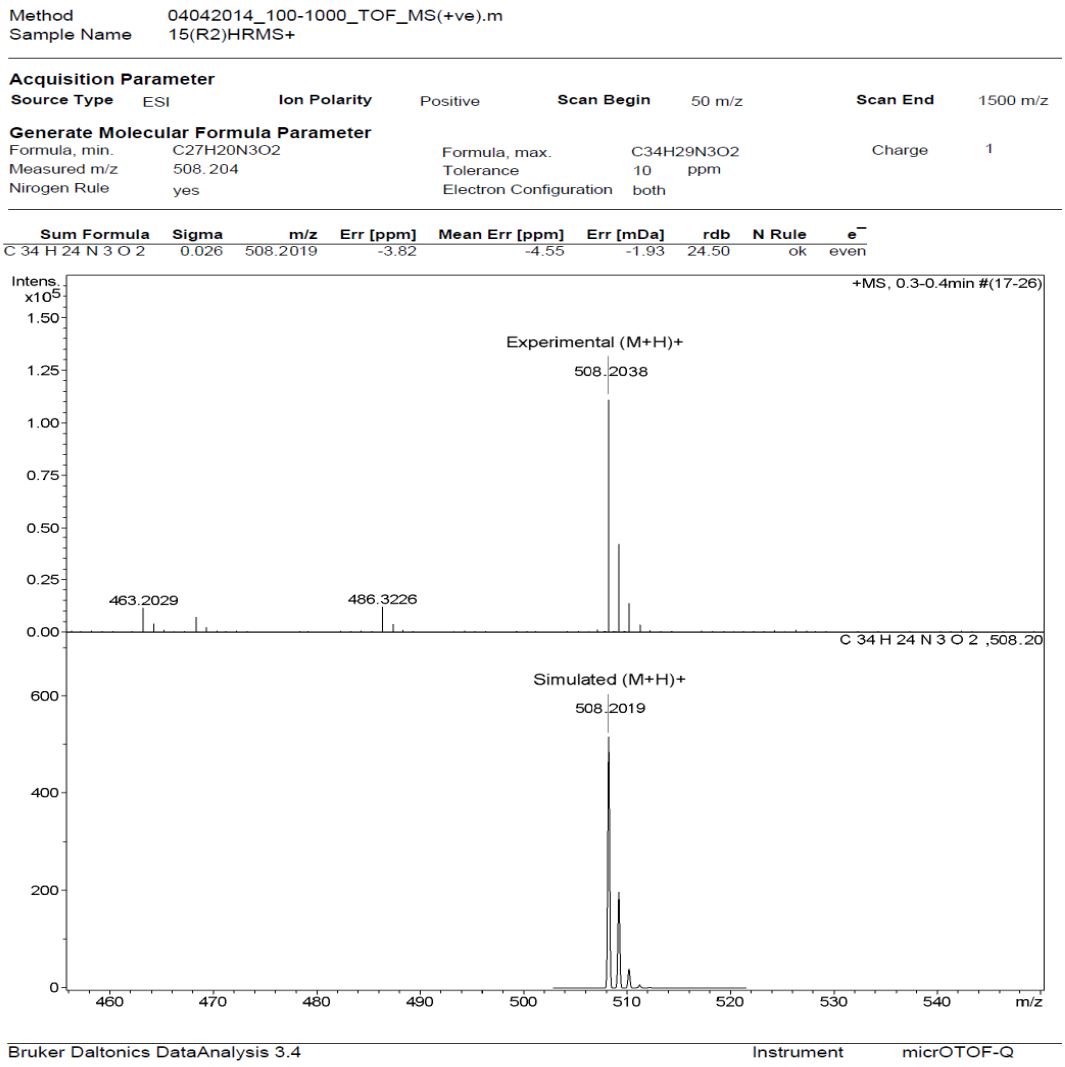

Figure S11: HRMS spectrum of **3**.

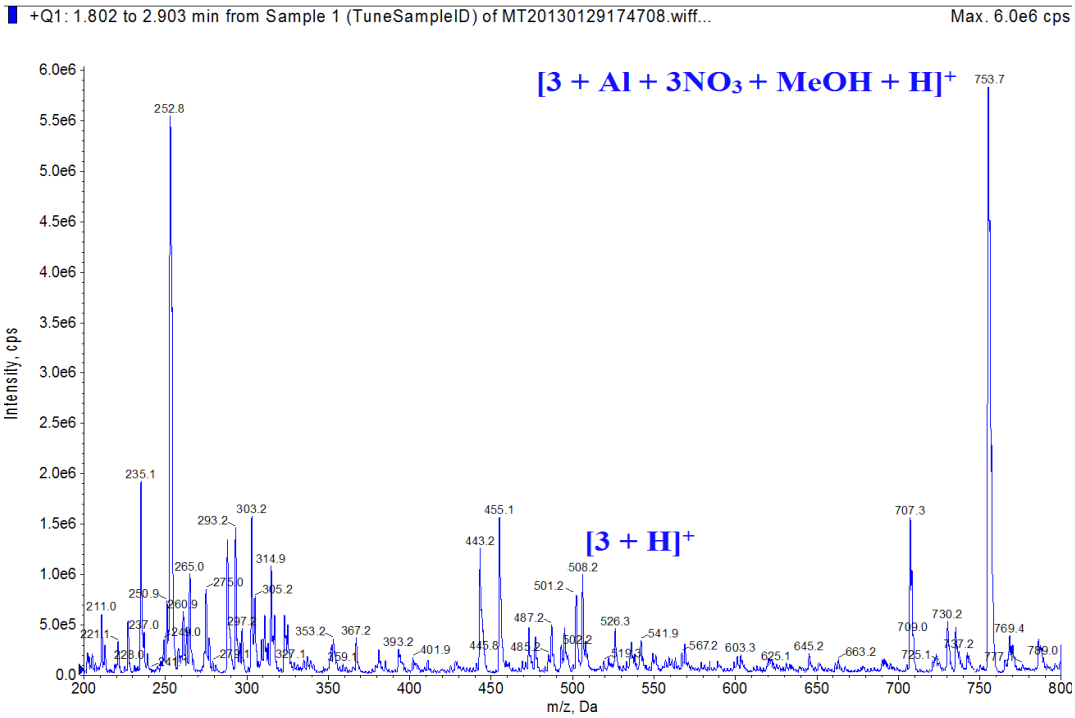

Figure S12: Mass spectrum of **3**+Al^{3+} complex.

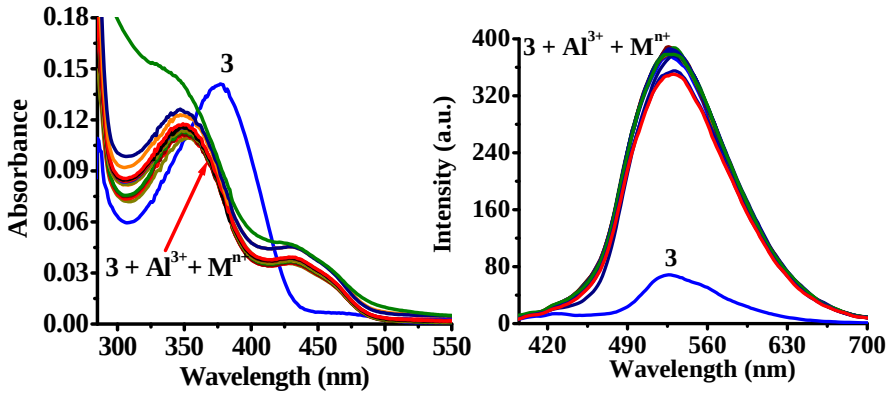

Figure S13: (a) Absorption and (b) emission spectra of interference studies upon addition of tested metal ions to a solution of **3**+Al^{3+} (10 μM) in HEPES buffer (v/v = 50%, pH 7.04).

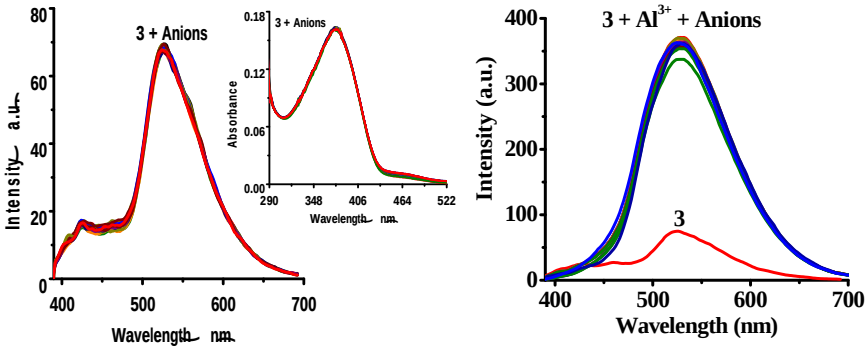

Figure S14: (a) Emission and Absorption (inset) spectra of **3** (10 μM) upon interaction of various anions (50.0 equiv) in HEPES buffer (v/v = 50%, pH 7.04). (b) Emission spectra of interference studies upon addition of different anions to a solution of **3**+Al^{3+} (10 μM) in HEPES buffer (v/v = 50%, pH 7.04).

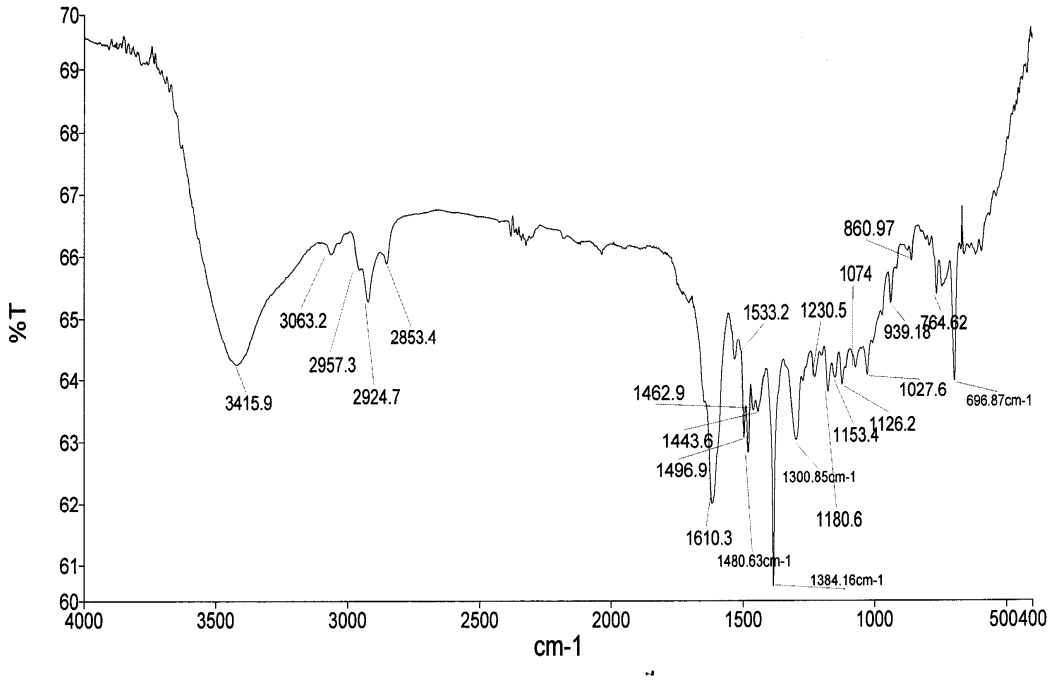

Figure S15: FT-IR spectrum of **3**+Al^{3+} complex.

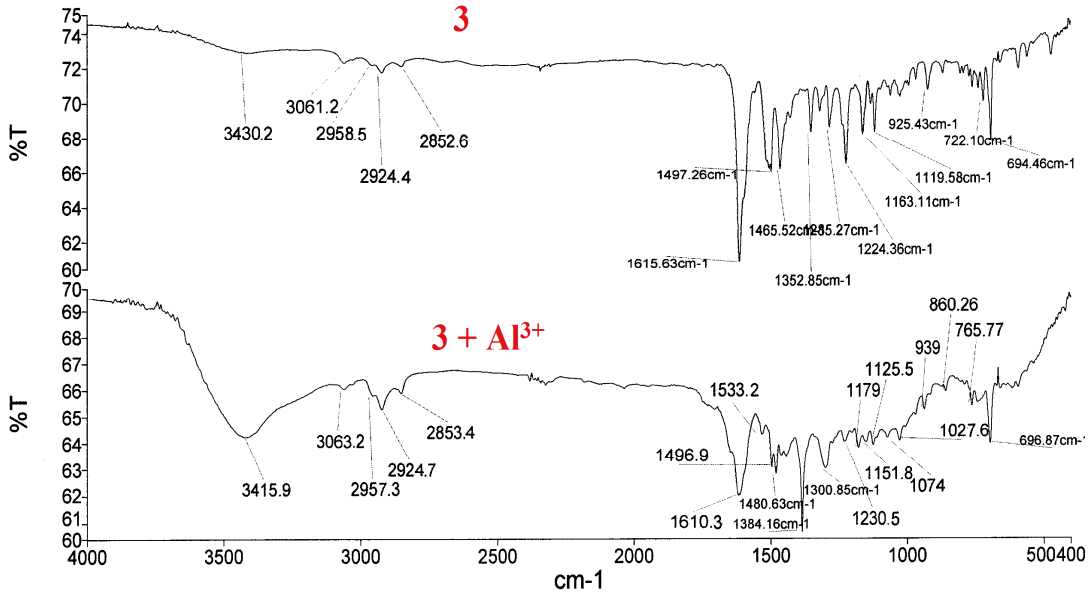

Figure S16: Stacked FT-IR spectrum of **3** and **3+Al^{3+}** complex.

Table S1: Photophysical properties of probe **3** and **3+Al^{3+}** in different solvents and water gradient systems

Solvents	**Water contents (vol %)**	**λ_{em} (nm)**		**Enhanced emission (in fold)**	**Quantum yield (Φ)**		**Enhanced Quantum yield (in fold)**
		3	**3+Al^{3+}**		**3**	**3+Al^{3+}**	
Benzene	0	432	434	5	0.004	0.011	2.75
CCl_4	0	432	434	5	0.003	0.01	3.33
CH_2Cl_2	0	436	484	14	0.009	0.043	4.77
Dioxane	0	530	506	11	0.0029	0.044	15.77
	10	530	508	13	0.0044	0.086	19.54
	20	530	516	8	0.0048	0.072	15
	30	530	530	7	0.005	0.061	12.2
	40	530	532	8	0.0059	0.077	13.05
	50	530	532	8	0.006	0.084	14
	60	528	536	8	0.0054	0.092	17
	70	526	536	8	0.004	0.051	12.75
THF	0	528	466	22	0.0028	0.068	24.28
	10	528	502	10	0.0043	0.088	20.46
	20	530	504	7	0.0045	0.07	15.55
	30	528	514	6	0.005	0.067	13.4
	40	528	526	6	0.0054	0.063	11.66
	50	528	528	6	0.006	0.07	11.66
	60	530	530	5	0.007	0.059	8.42
	70	530	530	5	-	-	-
ACN	0	532	546	5	0.0018	0.015	8.33
	10	530	546	3	0.0021	0.033	15.71
	20	526	538	5	0.0027	0.054	20

	30	526	530	8	0.0029	0.07	24.13
	40	526	532	10	0.0035	0.078	22.28
	50	524	534	11	0.0038	0.083	21.84
	60	522	536	13	0.004	0.046	11.5
	70	536	536	14	0.0019	0.027	14.21
EtOH	0	524	532	6	0.01	0.102	10.2
	10	524	533	7	0.098	0.108	1.10
	20	522	530	7	0.097	0.125	1.28
	30	522	530	7	0.097	0.109	1.12
	40	522	532	7	0.098	0.109	1.11
	50	524	532	7	0.008	0.087	10.87
	60	526	532	8	0.0068	0.094	13.82
	70	527	532	9	0.0076	0.067	8.81